UNIVERSITY OF TURKU

ON OPTIMAL USE OF RADIATION IN CARDIOLOGICAL PROCEDURES

Jukka Järvinen

TURUN YLIOPISTON JULKAISUJA – ANNALES UNIVERSITATIS TURKUENSIS
SARJA - SER. D OSA - TOM. 1489 | MEDICA - ODONTOLOGICA | TURKU 2020

UNIVERSITY OF TURKU

ON OPTIMAL USE OF RADIATION IN CARDIOLOGICAL PROCEDURES

Jukka Järvinen

TURUN YLIOPISTON JULKAISUJA – ANNALES UNIVERSITATIS TURKUENSIS
SARJA - SER. D OSA – TOM. 1489 | MEDICA – ODONTOLOGICA | TURKU 2020

University of Turku

Faculty of Medicine
Cardiology and Cardiovascular Medicine
Doctoral Programme in Clinical Research

Supervised by

PhD Joanna Sierpowska
Department of Physics
University of Kuopio
Finland

PhD Teemu Siiskonen
Radiation Dosimetry
Radiation Protection Centre
Finland

Professor Mika Teräs
Department of Physics
University of Turku
Finland

Reviewed by

Professor Hilde Bosmans
Imaging and Pathology
Catholic University of Leuven
Belgium

PhD Christelle Huet
Medical Physics
Institut de Radioprotection et de Sûreté
Nucléaire (IRSN)
France

Opponent

Docent Paula Toroi
Medical Radiation Physicist - SSDL
Office, IAEA
Austria

The originality of this publication has been checked in accordance with the University of Turku quality assurance system using the Turnitin OriginalityCheck service.

ISBN 978-951-29-8068-0 (PRINT)
ISBN 978-951-29-8069-7 (PDF)
ISSN 0355-9483 (Print)
ISSN 2343-3213 (Online)
Painosalama, Turku, Finland 2020

To the light of my life
All of you
Thank you

UNIVERSITY OF TURKU
Faculty of Medicine
Cardiology and Cardiovascular Medicine
JUKKA JÄRVINEN: On Optimal Use of Radiation in Cardiological Procedures
Doctoral Dissertation, 121 pp.
Doctoral Programme in Clinical Research
May 2020

ABSTRACT

In this thesis, the use of radiation in contemporary interventional cardiology (IC) has been investigated. The focus of the study is on patient doses in various minimally invasive procedures with higher doses. Patient exposure to radiation can be measured with Kerma area product (KAP) and its diagnostic reference levels (DRLs), maximum skin dose (MSD) and absorbed organ doses. In this thesis, all three doses are explored with accurate and repeatable methods and curiosity toward the causes behind the dose level variation.

KAP results show that the highest patient doses in IC occur in transaortic valve implantations (TAVIs) and percutaneous coronary interventions (PCI) with significant variation between hospitals and countries. In TAVIs, this variation is partly due to the novelty of the procedure, but in PCIs, the need for difficulty levels in the DRLs is apparent. The machine learning methodology used in this thesis provides insight into how such difficulty levels can be determined and what kinds of features they should be comprised of.

The MSD measurements performed with Gafchromic films show significantly higher dose levels in TAVIs than in other procedures and KAP and air kerma alert levels were proposed accordingly in Publication 3 of this thesis. The MSD levels show a high variance between hospitals and local DRLs were calculated for two of the participating hospitals. With the observed variation in respect to both KAP and air kerma, a good alternative to these alert levels are automatic skin dose estimations provided by the angiosystem manufacturers. In this work, two such algorithms were compared to the measured doses and the results were very promising.

Heart organ dose was measured with radiophotoluminescence (RPL) dosimeters and an anthropomorphic phantom in both a computed tomography (CT) scan routinely performed before a TAVI procedure and in a typical TAVI procedure. The results show that a majority of the dose is caused by the CT scan and that the dose from the procedure is relatively low compared to other published results.

In total, the thesis illustrates good investigative practices in radiation protection, their application to IC and results that benefit both contemporary cardiology and physicists working in the field.

KEYWORDS: Radiation dose, cardiology, optimization

TURUN YLIOPISTO
Lääketieteellinen tiedekunta
Kardiologia ja kardiovaskulaarilääketiede
JUKKA JÄRVINEN: Säteilyn optimaalisesta käytöstä kardiologiassa
Väitöskirja, 121 s.
Kliininen tohtoriohjelma
kesäkuu 2020

TIIVISTELMÄ

Tässä väitöskirjassa on tutkittu säteilynkäyttöä tämän päivän invasiivisessa kardiologiassa (IC). Työn painopisteenä ovat olleet potilasannokset erinäisissä minimaalisesti kajoavissa toimenpiteissä, joissa käytetään suhteellisen paljon säteilyä. Potilasannoksia voidaan määrittää annoksen ja pinta-alan tulolla (KAP) sekä sille asetetuilla vertailutasoilla (DRL), maksimaalisilla ihoannoksilla (MSD) sekä absorpoituneilla elinannoksilla. Tässä väitöskirjassa mitattiin näitä kolmea annosta tarkoilla ja toistettavilla tavoilla.

KAP tulokset osoittavat, että suurimmat potilasannokset aiheutuvat aorttaläppäproteesin katetriteitse tapahtuvassa asennuksessa (TAVI) sekä koronaarisuonten pallolaajennuksissa (PCI). Sekä TAVI- että PCI-toimenpiteissä voidaan havaita suurta vaihtelua sairaaloiden ja maiden potilasannoksissa. TAVI-toimenpiteissä havaittava vaihtelu liittyy osin toimenpiteen uutuuteen, mutta PCI-toimenpiteissä havaittava vaihtelu osoittaa tarpeen määrittää vertailutasot toimenpiteiden vaikeustasojen mukaan. Tässä työssä käytetty koneoppivaa algoritmia hyödyntävä metodologia auttaa hahmottamaan, miten vaikeustasot voi määrittää ja mitä asioita niiden tulisi ottaa huomioon.

Gafchromic-filmeillä tehdyt MSD-mittaukset osoittivat TAVI-toimenpiteissä olevan selkeästi muita toimenpiteitä isommat ihoannokset. Tämän johdosta TAVI-toimenpiteille asetettiin osajulkaisussa KAP- ja ilmakerma-hälytysrajat. Erityisesti kahdessa osallistuneista sairaaloista annokset olivat suuria ja niille ehdotettiin paikallisia sairaalakohtaisia hälytysrajoja. Suhteessa KAP- ja ilmakerma-annoksiin MSD-annosten vaihtelu oli hyvin suurta ja hyvä vaihtoehto hälytysrajoille ovatkin angiolaitevalmistajien algoritmit ihoannosestimaateille. Tässä työssä verrattiin näistä algoritmeista kahta ja tulokset olivat hyvin lupaavia.

Sydämen elinannoksia mitattiin radiofotoluminesenssidosimetrialla ja antropomorfisella fantomilla rutiinisti ennen TAVI-toimenpidettä tehtävässä tietokonetomografiakuvauksessa (CT) sekä tyypillisessä TAVI-toimenpiteessä. Tulokset osoittavat, että CT-kuvauksesta aiheutuva annos on toimenpiteen annosta suurempi ja toimenpiteen annos on julkaistuihin tutkimuksiin verrattaessa varsin pieni.

Kokonaisuudessaan väitöskirja havainnollistaa hyviä säteilysuojelun tutkimuskäytäntöjä, niiden soveltamista invasiiviseen kardiologiaan sekä tuloksia, jotka hyödyttävät sekä tämän päivän kardiologiaa että fyysikoita, jotka työskentelevät alalla.

AVAINSANAT: Säteilyannos, kardiologia, optimointi

Table of Contents

Abbreviations 8

List of Original Publications 10

1 Introduction 11

2 Review of the Literature 13
- 2.1 Cardiological diseases and angiographic procedures 13
  - 2.1.1 Coronary diseases and their treatment 14
  - 2.1.2 Arrhythmias and their treatment 15
  - 2.1.3 Structural malfunctions and their treatment 17
- 2.2 Use of radiation in cardiology 18
  - 2.2.1 Physical properties of radiation and its biological risks 19
  - 2.2.2 Optimizing the use of radiation 22
  - 2.2.3 Diagnostic reference levels 22
  - 2.2.4 Maximum skin dose dosimetry and alert levels 24
  - 2.2.5 Organ dosimetry 25
  - 2.2.6 CT imaging 26
- 2.3 Big data and data mining 27

3 Aims 28

4 Materials and Methods 29
- 4.1 Patient KAP doses 29
  - 4.1.1 Finnish and European DRLs 29
  - 4.1.2 Statistical and machine learning analyses 30
- 4.2 Patient skin dose measurements 35
- 4.3 Heart organ dose measurements 38

5 Results 42
- 5.1 Patient KAP doses 42
  - 5.1.1 Finnish and European DRLs 42
  - 5.1.2 Features and parameters predicting KAP dose 49
- 5.2 Patient skin doses 53
  - 5.2.1 Measured skin doses and alert levels 53
  - 5.2.2 Commercial skin dose mapping tools 55
  - 5.2.3 Uncertainty analysis 56
- 5.3 Heart organ doses related to TAVI 57

6 Discussion 59
- 6.1 Published diagnostic reference levels 59
- 6.2 Predicting features and difficulty levels 61

6.3 Patient skin doses 62
6.4 Heart organ doses related to TAVI 63
6.5 Future prospects of radiation use in cardiology 64

7 Summary/Conclusions 66

Acknowledgements 67

References 68

Original Publications 77

Abbreviations

ACC/AHA	American College of Cardiology/American Heart Association
AI	Apical introducer
Air kerma	Kinetic energy released per unit mass in air
AP	Anterior-posterior
AVNRT	Atrioventricular nodal re-entry tachycardia
BSS	Basic safety standards
CA	Coronary angiogram
CABG	Coronary artery bypass grafting
CH	Central hospital
CI	Confidence interval
CINE	cineangiography
CONCERT	European Joint Programme for the Integration of Radiation Protection Research
CRT	Cardiac resynchronization therapy
CT	Computed tomography
CTDIvol	CT dose index (volume)
CTA	CT angiography
DLP	CT dose length product
DRL	Diagnostic reference level
ECG	Electrocardiogram
EF	Electrophysiological procedures
ESC	European Society of Cardiology
EURADOS	European Radiation Dosimetry Group
FL	Fluoroscopy
FOV	Field of view
FFR	Fractional flow reserve
FREG	F-value regression
FT	Fluoroscopy time
Gy	Gray
IAEA	International Atomic Energy Agency
IC	Interventional cardiology
IEC	International Electrotechnical Commission
IVUS	Intravascular ultrasound
KAP	Kerma area product
kV	Kilovolt
LAO	Left anterior oblique
LAT	Lateral
mAs	Milliamperesecond

MEDIRAD	Implications of Medical Low Dose Radiation Exposure
MIR	Mutual information regression
MOSFET	Metal oxide semiconductor field effect transistor
MSD	Maximum skin dose
MSE	Mean squared error
MSURF	MultiSURF
MSURFS	MultiSURFstar
NA	Not applicable
NRD	Net reflective density
OCT	Optical coherence tomography
OID	Object image distance
P_{KA}	Product of kerma and area, KAP
PC	Pigtail catheter
PCI	Percutaneous coronary intervention
PEAR	Pearson correlation coefficient
PET	Positron emission tomography
PI	Pacemaker implantation
RAO	Right anterior oblique
RBF	Radial basis function kernel
RELF	ReliefF
RF	Radiofrequency
ROI	Region of interest
RPAK	Reference point air kerma
RPL	Radiophotoluminescence
RQR	Radiation quality of radiation beam
SID	Source image distance
SOD	Source object distance
SPEA	Spearman's correlation coefficient
SURF	SURF
SURFS	SURFstar
Sv	Sievert
SVR	Support vector regression
STUK	Säteilyturvakeskus, Radiation and Nuclear Safety Authority of Finland
TAVI	Transaortic valve implantation
TLS	Thermoluminescence dosimetry
TPW	Temporary pacing wire
TOE	Transoesophageal echo
UH	University hospital
US	Ultrasound
VERIDIC	Validation and estimation of radiation skin dose in interventional cardiology

List of Original Publications

This dissertation is based on the following original publications, which are referred to in the text by their Roman numerals. In addition, the thesis contains unpublished results on patient organ dosimetry.

I Järvinen J, Sierpowska J, Siiskonen T, Järvinen H, Kiviniemi T, Rissanen T, Matikka H, Niskanen E, Hurme S, Larjava HRS, Mäkela TJ, Strengell S, Eskola M, Parviainen T, Hallinen E, Pirinen M, Kivelä A, Teräs M. Contemporary Radiation Doses in Interventional Cardiology: a Nationwide Study of Patient Doses in Finland. Radiation Protection Dosimetry, 2019; 1-11, ncz041.

II Siiskonen T, Ciraj-Bjelac O, Dabin J, Diklic A, Domienik-Andrzejewska J, Farah J, Fernandez JM, Gallagher A, Hourdakis CJ, Jurkovic S, Järvinen H, Järvinen J, Knežević Ž, Koukorova C, Maccia C, Majer M, Malchair F, Riccardi L, Rizk C, Sanchez R, Sandborg M, Sans Merce M, Segota D, Sierpowska J, Simantirakis G, Sukupova L, Thrapsanioti Z, Vano E. Establishing the European diagnostic reference levels for interventional cardiology. Physica Medica, 2018, 54: 42-48.

III Järvinen J, Sierpowska J, Siiskonen T, Järvinen H, Kiviniemi T, Rissanen T, Matikka H, Niskanen E, Hurme S, Larjava HRS, Mäkela TJ, Strengell S, Eskola M, Parviainen T, Hallinen E, Pirinen M, Kivelä A, Teräs M. Contemporary Radiation Doses in Interventional Cardiology: a Nationwide Study of Maximum Skin Doses in Finland. Radiation Protection Dosimetry, 2019; 1-10, ncz273.

IV Suomi V+, Järvinen J+, Kiviniemi T, Ylitalo A and Pietilä M. Exhaustive feature selection for predicting KAP radiation dose in coronary angiographies and percutaneous coronary interventions. Computers in Biology and Medicine, 2020; 120, 103725.
+These authors contributed equally to this work.

1 Introduction

The use of radiation in medicine is common and its uses are both numerous and highly variable (STUK, 2019). Many of the current uses are ionizing, which means that their use causes harm and is carefully regulated. One of the most intensive uses of radiation in medicine occurs during long angiographic procedures (Wall and Hart, 1997) that generally diagnose problems with minimally invasive techniques. In interventional cardiology (IC), all procedures have either a diagnostic or therapeutic function and are becoming more and more numerous and complex (Blackledge and Squire, 2009; Fokkema et al., 2013; Kiviniemi et al., 2016).

The cardiological use of radiation is generally considered to be well-justified with immense and direct benefits, but not entirely without issues with optimization (e.g. Picano and Vano, 2011). With multiple diseases that can be diagnosed with life-saving or changing implications, there is no question as to the value of using radiation in IC, but the question of how much should be used is one that can never be entirely solved. Optimizing use of radiation in IC diminishes risks of cancer and skin damage for the patient as well as for the cardiologists, radiographers and nurses in the angioroom. With an ageing patient population and changes in work habits and technology, optimization in IC is currently more important than ever.

Internationally, interest in radiation doses in cardiological procedures continues to be enthusiastic (Klein et al., 2009; Knuuti and Järvinen, 2014; Sun et al., 2013) and there have been multiple studies on dose optimization in cardiological procedures (Klein et al., 2009; Rehani, 2007). With sufficient, easily accessible information such as distributed and readily available guidelines, this concern is developing into a more robust culture of dose hygiene – one with regular quality assurance and dose optimization from both technological and practical aspects. Concurrently with this work, such guidelines were prepared by the Radiation and Nuclear Authority in Finland (STUK) (Järvinen et al., 2018a).

In this thesis, the contemporary practice of cardiological use of radiation in angiographic procedures is explored. In particular, patient stochastic and deterministic risks, as well as possible ways of minimizing them without impacting patient safety in terms of complications are delved into. The thesis comprises four different publications on patient Kerma area product (KAP), features predicting them, skin doses and unpublished results on patient organ (heart) dosimetry in a CT heart scan and a TAVI procedure. In the following review of literature (Chapter 2), relevant concepts such as central cardiological procedures and factors that affect the use of radiation in them are introduced. In the later chapters, the aims of the study (Chapter 3), the collected data and methods (Chapter 4), results (Chapter 5), discussion (Chapter 6), and conclusions (Chapter 7) are presented.

2 Review of the Literature

2.1 Cardiological diseases and angiographic procedures

The most common cardiological diseases that are diagnosed and, to an extent, treated with procedures, comprise of coronary diseases, arrythmias or electrophysiological diseases and structural malfunctions, such as in the valve (Steinberg et al., 2010). Relatively recently, many cardiological procedures have become increasingly common (Blackledge and Squire, 2009; Fokkema et al., 2013; Kiviniemi et al., 2016).

In an IC procedure, patients are diagnosed or treated using fluoroscopy guided methods. Commonly, the procedure is performed using either femorally or radially inserted catheters, which are then imaged and used for various diagnostic and treatment purposes. During the procedure, the patient is imaged with fluoroscopy and Cine series with the cardiologist and assistant typically standing right next to them. A photo of an angioroom in Turku Heart Centre is shown in Figure 1. In general, the procedures are minimally invasive but, if necessary, they can be changed to surgical procedures. Pacemaker implantations form an excemption as they require minor surgery.

Cardiological diseases are treated with multiple methods with drug treatment being the most common and surgery being reserved only for patients for whom other treatments are not sufficient. Focus is also traditionally given to providing guidance on how to live healthy to increase quality of life; specifically the European Society of Cardiology (ESC) lists the following lifestyle choices as factors that significantly lower the risk of cardiological disease (ESC, 2012):

- No use of tobacco.
- Adequate physical activity: at least 30 minutes ve times a week.
- Healthy eating habits.
- No overweight.
- Blood pressure below 140/90 mmHg.
- Blood cholesterol below 5 mmol/L (190 mg/dL).

- Normal glucose metabolism.
- Avoidance of excessive stress.

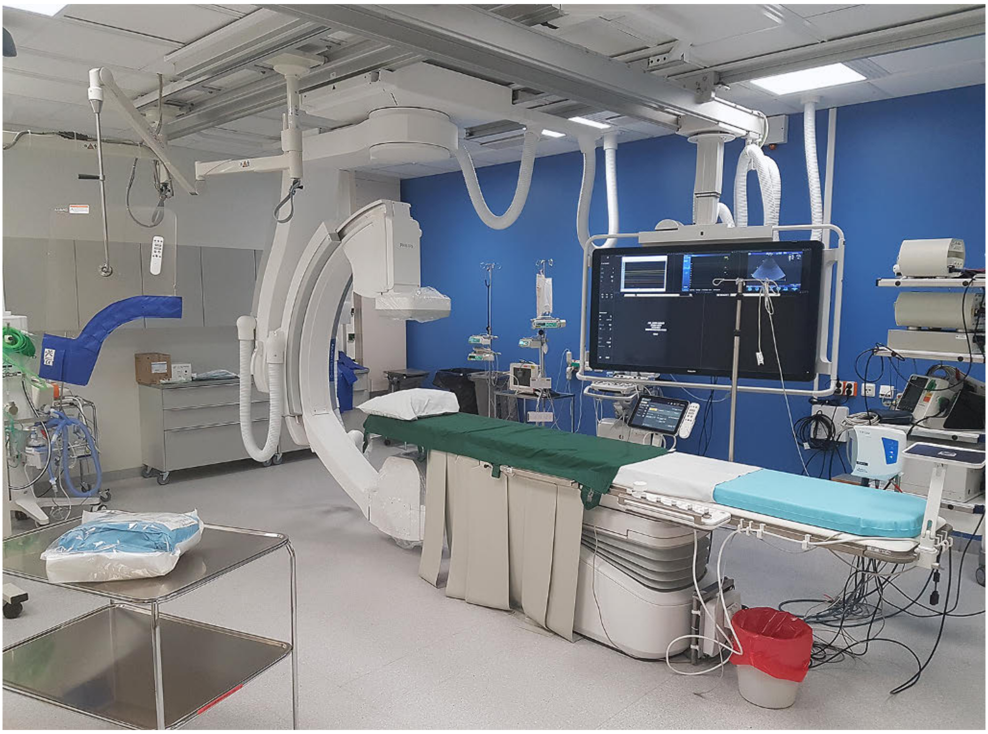

Figure 1. Photo of an angioroom in Turku Heart Centre. The room has capabilities for coronary, electrophysiological and TAVI procedures as well as pacemaker implantations. Inside the room, there are multiple radiation shields for personnel. The angiodevice in the photo is Philips Azurion 7 C 12.

2.1.1 Coronary diseases and their treatment

Coronary disease is the most common cause for cardiological procedures. In a coronary disease, occlusion in the coronary arteries causes insufficient blood flow, which can cause a lack of oxygen in the heart tissue, leading to an infarction (Ashley and Niebauer, 2004). Occlusions can often be diluted with drugs, but if their effect is not sufficient, the patient eventually undergoes a coronary angiography (CA). During CA, blood flow in the coronaries is diagnosed in pulsed X-ray imaging with a suitable iodine-based contrast agent to enhance visibility of blood flow in the coronaries. If the patient's diagnosis requires it, CA is often immediately followed by percutaneous coronary intervention (PCI), in which stenotic or occluded coronaries are cleared or expanded with a balloon or other stenting device as illustrated in Figure 2. PCI can be performed immediately (ad hoc) or electively. The alternative to PCI is bypass surgery (CABG), which is considered superior in multivessel occlusions, but it carries more significant risks due to its invasive nature (Sipahi et al., 2014).

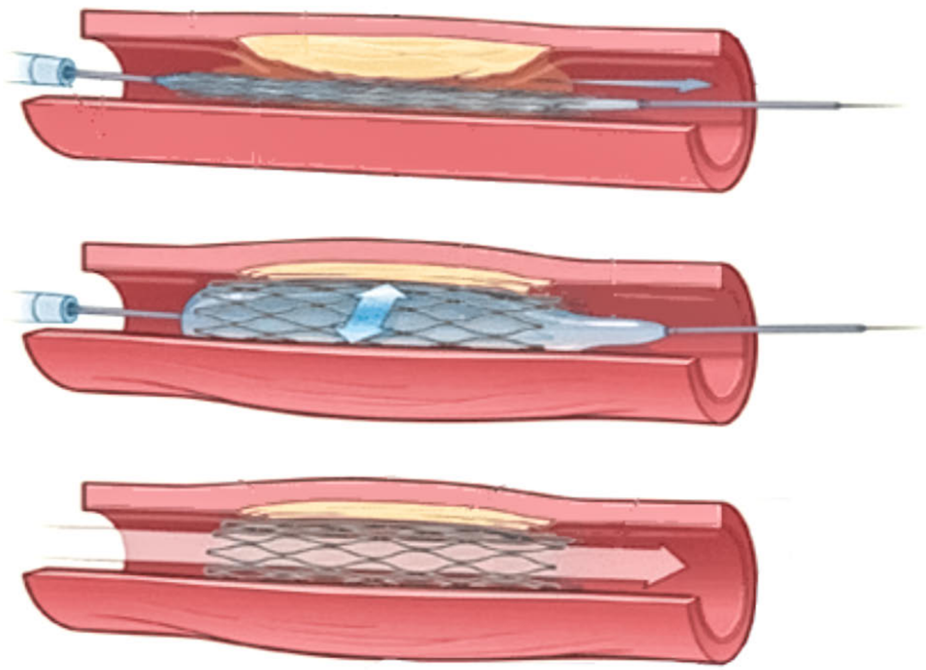

Figure 2. Illustration of percutaneous coronary intervention in a stenotic coronary artery. The stent is placed at the stenotis and the inserted balloon is inflated and retrieved. After three months from the procedure, blood flow is normalized (Oberhauser et al., 2009).

2.1.2 Arrhythmias and their treatment

Arrhythmias, or abnormal heart rhythms, are caused by changes in the sequence of the heart's electrical impulses. Most arrhythmias are not treated, as they do not pose a signicant threat or harm to the quality of life. To varying extents, arrhythmias can be treated with medication, electrophysiological procedures or pacemakers. One of the main motivations to increasingly treat them is that they have been recognized to increase stroke risk (Engström et al., 2000). Treatment is chosen on an individual basis based on multiple factors, but it can be briefly summarized as being mainly dependent on the type of arrhythmia, frequency and duration of attacks and patient age and condition.

X-ray-guided electrophysiological procedures are performed for only select types of arrhythmias that can be dangerous if the patient develops or has a coronary disease. The procedures generally consist of surface and intracardiac ECG monitoring, triggering of the arrhythmia, and its treatment. Intracardiac ECG is performed by guiding catheters into the right atrium, coronary sinus, HIS bundle, and the apical right ventricle (Josephson, 2008). Once the catheters are in place, arrhythmia is induced by burdening the heart with fast pacing. If the arrhythmia begins, its origin and pathways can be determined. Within the pathways, electrical impulses circulate and cause the muscles to contract and induce the arrhythmia.

Arrhythmia's treatment can generally be either lifestyle guidance, medicinal or electrical cardioversion, or a suitable procedure. An increasingly common treatment is ablation, in which critical pathways for the electrical signal are ablated with a (radiofrequency) RF-catheter or a heat-absorbing cryoablation catheter in direct contact with the tissue. These techniques provide comparable results, and for the physician, the main differences are in the ease of use and size of the ablation area. (Kuck et al., 2016)

Atrioventricular nodal re-entry tachycardia (AVNRT) is a supraventricular tachycardia, which means that it originates above the HIS bundle and causes an abnormally high heart rate. AVNRT is caused by the circulation of an electrical impulse in or around atrioventricular node, which is created by a reentry circuit as the impulse travels in two pathways at varying speeds. AVNRT, if especially frequent or combined with coronary disease, can require catheter ablation. (Cadogan, 2014; Haissaguerre et al., 1989)

Atrial flutter is a supraventricular tachycardia that is caused by a reentry circuit in the right atrium. The resulting tachycardia is typically within 200-400 bpm. As with AVNRT, the other pathway can be cut with ablation. (Daoud and Morady, 1998; Lee et al., 2005)

Pacemaker implantations, as the term implies, refer to installations of various kinds of pacemakers. All types of pacemakers significantly impact patient's quality of life and are typically the last non-conservative treatment offered for arrhythmias. The most common kinds are one and two chamber pacemakers (Furman et al., 1989, p.261). During an implantation, leads are taken to the right ventricle, right atrium, or both. The leads measure and deliver electrical signals from these locations to the device, which is typically implanted under the skin in the chest, below the collar bone. It is programmed to perform in accordance with the patient's own rhythm, with various possibilities for sensing and therapy. Typically, radiation is only needed to guide the implantation and document various stages of the procedure.

Implantation of biventricular Cardiac Resynchronization Therapy (CRT) devices is often considered significantly more challenging as an additional lead is taken into the coronary sinus for left ventricular pacing (Airaksinen et al., 2016, p.748). CRT's are implanted in a case of more severe heart failure where both ventricles need to be paced for synchronized functioning.

2.1.3 Structural malfunctions and their treatment

Although the definition is relatively new [introduced in 1999 by Martin Leon (Steinberg et al., 2010)], structural heart diseases comprise a number of various diseases. The most novel and, as such, perhaps the most important procedures in the IC use of radiation are transaortic valve implantations (TAVI) (Airaksinen et al., 2016, p.833), which consist of implanting a prosthetic aortic valve with a catheter to replace a malfunctioning valve. Typically, the malfunction is caused by severe aortic stenosis. The prosthesis can be placed using various approaches. In the transapical approach, the left ventricular apex is located using angiography, an incision is made close to the apex of the heart, and the pericardium is punctured. The valve is then inserted with an introducer and opened, e.g., with an inflatable balloon (Cheung and Lichtenstein, 2012). Opening a TAVI prosthesis is shown in Figure 3.

Another common TAVI approach is transfemoral (Cribier et al., 2009), in which the catheter is guided to the aortic valve via the femoral artery. Due to its less invasive nature, it is preferred to the transapical approach when possible (Bapat et al., 2012). However, the need for fluoroscopy is often significantly higher, and there can be problems with visibility of the prosthesis. A third common technique is transaortic, in which the valve is guided through the ascending aorta (Bapat et al., 2012).

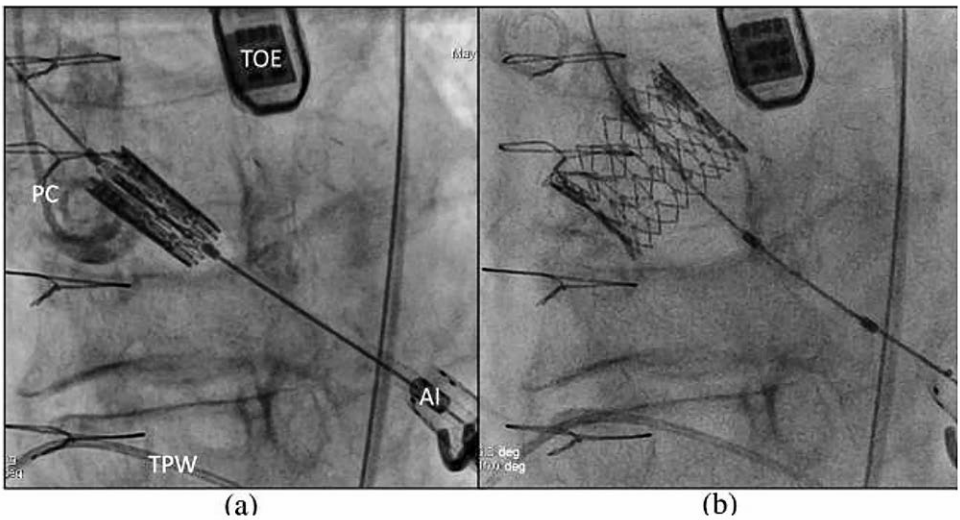

Figure 3. Opening of a TAVI prosthesis. (a) Collapsed stent over a guidewire via the apical introducer (AI). A pigtail catheter (PC) can also be seen in the aortic root, in addition to a right ventricular, temporary pacing wire (TPW) and a transoesophageal echo (TOE) probe. (b) The expanded prosthesis in place. (Clayton et al., 2013).

Other structural malfunctions that can be treated with minimally invasive procedures include, for example, the treatment of mitral valve stenosis (Chmielak et al., 2017) or regurgitation (Sherif et al., 2016) and left atrial appendage occlusion to prevent the formation of thrombus (Lund et al., 2012). These procedures are mainly ultrasound-guided and, thus, the use of ionizing radiation in them is minimal.

2.2 Use of radiation in cardiology

The most important factor in how radiation is used in modern IC is enabling and assisting in various procedures and minimizing risk of complications, including those due to use of radiation itself. IC procedures are minimally invasive, and to succeed, they require a multitude of information on patient physiology and anatomy and procedure status. This information can, to an extent, be acquired with various techniques and devices such as electrocardiogram, ultrasound, esophageal ultrasound, intravascular ultrasound (Mantziari et al., 2011), infrared optical coherence tomography (Terashima et al., 2012) or fractional flow reserve for coronary blood pressure measurement (Mehra and Mohan, 2015), but for most cardiological procedures, good-quality X-ray images are essential.

The use of radiation in medicine has three basic principles: justification, optimization and dose limitation (ICRP, 2007). All use of radiation should have a realistic expected benefit that outweighs the harm caused by the radiation. In IC, cardiological diseases are first diagnosed using information collected with electrocardiograms (ECG), blood pressure tests, blood tests, US, computer tomography (CT) or isotope imaging such as positron emission tomography (PET) (Camm et al., 2009). This vast amount of information translates to the careful assessment of each procedure's justification: risks of various complications, cancer or skin damage and probability of success.

In IC, patient radiation dose is measured with maximum skin dose (MSD) and KAP. MSD is defined as the maximum dose in a 1 cm^2 on the skin and, due to difficulties in measuring it, increasingly estimated during procedures. KAP on the other hand designates output radiation multiplied by irradiated area and is automatically either measured or calculated with precision mandated by law (Sosiaali- ja terveysministeriö, 2018). In angiodevices, KAP is typically calculated based on x-ray tube output parameters and field of view (FOV).

During IC procedures, contrast agent is utilized to increase visibility of arteries and veins, and radiation is used in pulses with either fluoroscopy (FL) or cineangiography (cine) modes. FL refers to low-dose and low-image quality placement of catheters and cine to series of images taken with significantly higher dose and better image quality. During procedures, cardiologists can vary pulse rate and choose from typically several templates of varying image quality and dose rate for the given procedure.

During cardiological procedures, the X-ray tube angle or projection is typically changed frequently for optimized visibility. This workflow results in multiple entry points for the radiation beam and significantly reduces the MSD. However, oblique or lateral projections increase the KAP, as more tissue needs to be penetrated. The effect on total KAP depends on improved visibility of the regions of interest (ROI).

Based on the size of the ROI, the x-ray field can also be collimated, or the ROI can be zoomed into. Whereas collimation limits the size of the irradiated area, the zoom also enlarges the image on the screen and increases its quality by increasing the amount of radiation used for generating it. How much zoom increases it depends mainly on how the angiosystem has been preprogrammed and the level of zoom.

Traditionally, fluoroscopy time (FT) has been used to describe the use of radiation in procedures. However, due to the difference in dose levels between cine and FL, the settings for image quality, zoom, collimation and projection choices, its effect on total KAP is complex, and its use as a diagnostic reference level (DRL) in angiographic procedures is no longer recommended by the International Commission on Radiation Protection (ICRP) (ICRP, 2017).

The use of radiation in cardiology is not entirely limited to IC. Especially with recommendations of CT angiographies (CTA) by the European Society of Cardiologists (ESC) (ESC et al., 2013), and with more and more prevalent PET imaging of the heart, a significant amount of radiation to the heart is delivered outside of angiorooms.

2.2.1 Physical properties of radiation and its biological risks

Harm to the patient can be divided into stochastically increased cancer risk (Lin, 2010), commonly calculated from the KAP and the risk of deterministic skin damage at the entry point of the radiation. Ionizing radiation has three possible scenarios when traveling in a medium: it can pass through, scatter or be absorbed. All three of these phenomena are dependent on the density of the matter and energy of the radiation. When radiation passes through a patient, it can be absorbed by the detector and becomes data in the resulting image. Contrast in the image is due to differences in the density of the matter, which affect the amount of absorbed and scattered radiation. When radiation is scattered, its path deviates, and amount of noise in the resulting image is increased. In addition, scattering is the reason that all facilities using radiation need to be shielded. This need for shielding also applies to all personnel present inside the shielded area while radiation is used, e.g., in procedures.

Radiation from an X-ray tube has a maximum energy controlled by tube voltage. An example of an energy spectrum for an X-ray tube with a typical tungsten cathode is illustrated in Figure 4. The more energy the X-ray photons have, the better they penetrate matter. Copper or aluminum filtration is used to absorb much of the lower-energy radiation and prevent it from reaching the patient, but nonetheless, a significant portion of radiation is absorbed at its entry point – the patient's skin. Besides radiation energy, MSD is affected by the procedure's total KAP and projections used in it. Whereas patient cancer risk is a statistical effect with a multitude of factors and relatively rare occurrence, patient skin damage due to MSD is a deterministic effect.

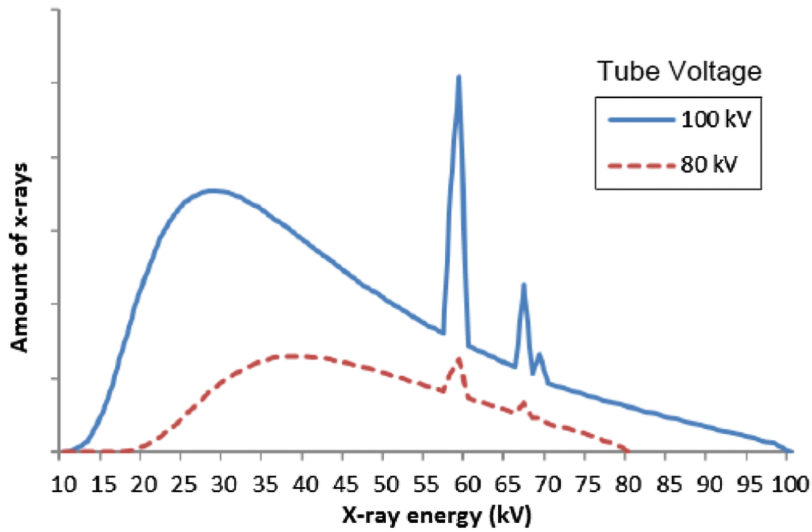

Figure 4. Illustration of radiation energy spectrum for a typical tungsten anode for 80 and 100 kV. The drop in the amount of x-rays at low energies is due to filtration.

When absorbed, energy from the radiation may cause molecule ionization, further causing physical and chemical reactions in the matter. In a cell, direct ionization or these indirect reactions can harm DNA strands, possibly causing the cell to mutate. For example, in a PCI procedure, the absolute increase in cancer risk is estimated to be roughly 0.02% for typical cardiological patients (Vijayalakshmi et al., 2007). Besides the procedure, a relative increase in cancer risk also accounts for patient age and gender, as illustrated in Figure 5. Cancer risk estimations with effective doses should not be used for individual purposes due to the imprecision of tissue weighting factors and the estimations included in them (Dietze et al., 2009; Fisher and Fahey, 2017).

Figure 6 depicts how the probability of patient harm depends on the dose received. According to the model shown, even small doses are assumed to increase cancer risk, whereas the deterministic skin damage has a clear threshold (Paile, 2002, Chapter 3). Commonly, this threshold is estimated as 2 Gy for early transient erythema (Balter et al., 2010).

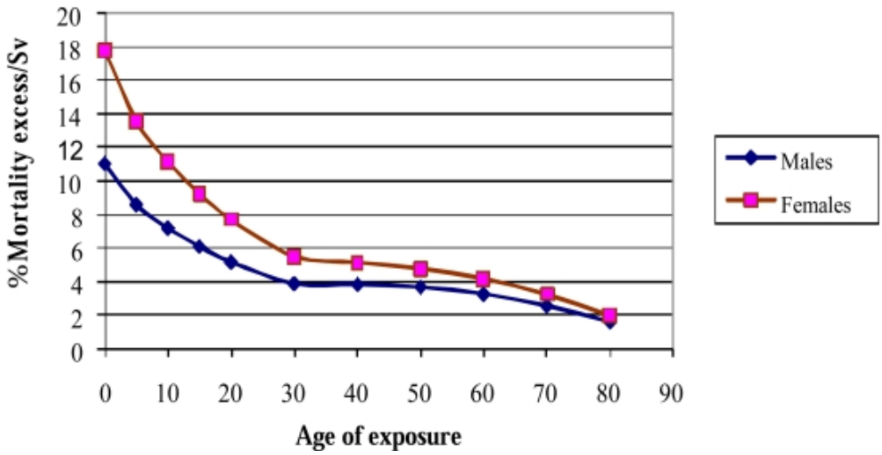

Figure 5. Illustration of age and gender dependency of cancer risk in radiological examinations and procedures (Foffa et al., 2009).

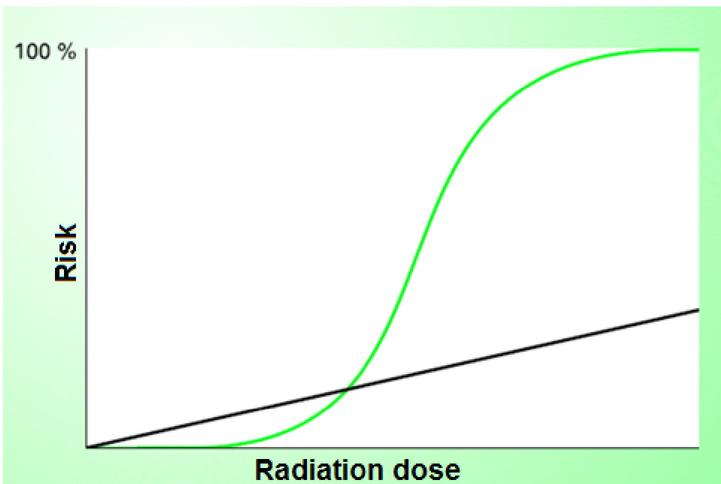

Figure 6. Illustration of how stochastic (black) and deterministic (green) harm to patient depend on dose level (Paile, 2002, Chapter 3).

2.2.2 Optimizing the use of radiation

As mentioned above, the use of radiation in medicine is commonly both justified and reasonably safe for the individuals in question. However, the use of radiation in medicine is never completely optimized. With a human being the final observer of the x-ray image, some level of subjectivity as to what constitutes sufficient image quality is always present. In cardiological procedures, optimization relies on multiple aspects of the procedures and is difficult to assess thoroughly (ICRP, 2007). Compared to diagnostic imaging, the use of radiation in procedures is always more situational and is based on instantaneous and learned continuous decisions. In addition to patient anatomy, hospital working habits and the physician's skill, what exactly is carried out in the procedure and procedure-specific physiological changes affect the need for FL and cine. For newer procedures such as TAVI, what steps are taken during the procedures is also liable to change with time (Kaier et al., 2017).

With a realistic view of the contemporary practice, necessary changes in the practice can be introduced. In cardiology, these changes can include the careful assessment of the cardiologists' working habits, optimization of the angiographic system's image quality or a more thorough assessment of the system's capability and functioning. The central aspects in all optimizations are the availability of relevant data and motivation of the personnel.

Optimizing radiation use in cardiological procedures can be measured, to an extent, by patient KAP. To optimize KAP and to know what level is realistically achievable, reference points are needed. These can be, and in some instances are, requested from other hospitals performing similar procedures, but diagnostic reference levels (DRLs) (ICRP, 2017) are preferable.

As stochastic risks from the use of radiation in IC procedures are typically considered to be justified and outweighed by the benefits of the procedure, consideration of the dose limitation under normal, accordingly optimized circumstances in IC is a serious concern, mainly with pregnant or young patients, along with procedures with significant risk of deterministic skin damage. However, with an increasing number and complexity of IC procedures, dose limitation should also be applied to staff due to their slow-but-steady exposure to small doses of radiation and associated cancer and cataract risks (Vano et al., 2010). Besides patient dose, staff doses are affected by numerous factors, such as the use of shielding, distance from the patient and projection. In Finland, guidelines for IC staff were published by the STUK in 2018 (Järvinen et al., 2018a).

2.2.3 Diagnostic reference levels

The recommended methodology to set DRLs is to gather a sufficient amount of data from multiple hospitals and take a third quartile of their medians (ICRP, 2017). This methodology can produce significantly lower levels than if the third quartile were taken from the total data (Georges et al., 2016).

Diagnostic Reference Levels (DRLs) offer a reliable basis for optimizing the use of radiation and are easy to rely on (ICRP, 2017). Historically based on dose surveys by the United Nations Scientific Committee on the Effects of Atomic Radiation (UNSCEAR), the concept of investigation levels was first proposed by ICRP in its 1990 recommendations (Wall et al., 1998). These days, the guidelines for DRLs are posed by the ICRP as recommendations, and their use is relatively free and manifold. In Finland, DRLs have traditionally been set by the STUK, but it is likely that some will be posed regionally by the EU in the future. Regional levels require significant international coordination and cooperation. As such, the involvement of either national or international organizations can be seen as a requirement, even if only for their network connections.

At the ground level, local DRLs also exist in many hospitals for various examinations and procedures, (Saukko et al., 2017, e.g.). Local DRLs cannot be higher than the existing national DRLs, and they apply only to the data from a specific hospital. However, they also offer valuable information and comparison material to other hospitals. In addition to national centers for radiation protection and ground-level hospitals, also the International Atomic Energy Agency (IAEA) utilizes the ICRP recommendations for basic safety standards and their better implementation.

Traditionally, DRLs serve to set a level of comparison for the current level of radiation used in diagnostic imaging. Despite some challenges related to larger variations, the same concept translates well to cardiac procedures. Setting a comparison point increases awareness about the issue and encourages action. DRLs set the organization up to aim for and assign resources to specific targets. In cardiology, realistic and specific DRLs and subsequent dose comparisons provide the cardiologists with incentives and regular reminders to be concerned about the radiation dose.

DRLs can be set for any numerical parameter relevant to a study or procedure, but generally, KAP is considered the most suitable for optimization purposes. For cardiological procedures in Finland, the first DRLs were KAP and FT levels set in 2006 for CA (60 $Gy \cdot cm^2$ and 8 min) and PCI (100 $Gy \cdot cm^2$ and 20 min) (STUK, 2005). Other contemporary DRL publications include the French 2nd RAY'ACT from 2017, which reported 26 $Gy \cdot cm^2$ DRL for CA and 60 $Gy \cdot cm^2$ DRL for PCI and the Swiss DRLs for CA (50 $Gy \cdot cm^2$), PCI (100 $Gy \cdot cm^2$), PI (5 $Gy \cdot cm^2$), electrophysiological procedures (EF, 20 $Gy \cdot cm^2$) and TAVI (100 $Gy \cdot cm^2$). Based on the data used in Publication I of this study, new DRLs were published in 2016 (STUK, 2016).

In recent years, some DRLs such as Finnish DRLs for childrens' CT examinations (STUK, 2015) have been published as a function of patient weight. The main motivation for this is the huge variation in children's size and the well-known relationship between patient size and the required amount of radiation; with bigger patients, more of the dose is absorbed and scattered, so more is needed for a good image quality. For interventional procedures, a similar variation is notable, but the cause is complex. For some time now, the ICRP has recommended the use of difficulty levels [the latest being (ICRP, 2017)] and this was one of the main motivations for Publication 1. For cardiological procedures, the difficulty of a PCI is described to some extent by the American Heart Association/American College of Cardiology (AHA/ACC) score for lesion classication (Ellis et al., 1988, 1990; Ryan et al., 1988), but no other procedures have such scores. The central criteria of the score are tortuosity of the vein, location, size and density of the thrombus and age of total occlusion. In addition, the AHA/ACC score's suitability for describing how much radiation is required is questionable.

With the perceived variation in procedure DRLs, the comparison to DRLs and their application should be handled with care. The possible exceeding should not be reacted to by altering of the image quality too much but rather by comparing the procedure methodology and the many aspects relevant to the procedures instead as an incentive to find out why the exceeding occurs and how dose optimization should be carried out.

2.2.4 Maximum skin dose dosimetry and alert levels

The radiation dose to patient skin can cause various levels of harm, depending mainly on the amount of radiation and its energy. Skin exposure limits and their assessment are mandated by the IAEA in its basic safety standards (BSS) directive (IAEA, 2014). As mentioned above, X-ray beam filtration significantly reduces skin dose. Deterministic harm to a cardiology patient's skin can be most reliably measured in 2D with reflective Gafchromic film dosimetry (Amano et al., 2002, 2003). Placed under the patient, these films absorb a slight amount of the passing radiation and darken with respect to how much radiation they absorb (Farah et al., 2015). After irradiation, films are scanned and the measured film darkening is compared to carefully produced calibration fits to obtain an estimate for the irradiated dose. The uncertainty of Gafchromic film dosimetry has been proposed to be 20% by Farah et al (Farah et al., 2015).

Gafchromic film accuracy requires careful calibration, maintenance and analysis of the films. As such, they are not suitable for clinical practice. Even so, they function as a gold standard for skin dosimetry and enable setting alert levels for KAP, so that routines can be formed for diminishing MSD, when the KAP alert level is exceeded.

Typically such action includes recommending projections which do not result in dose to the location of MSD, limiting the use of cineangiography (Cine) or, in extreme cases, resolving to continue the procedure at another date.

Contemporary evaluations of patient skin doses in cardiology are scarce and relatively old, ranging from 2003 to 2014. For PCI, mean and median skin doses range from 0.5 to 1.3 Gy. Very little data on TAVI skin doses have been published.

A novel method for skin dose estimation are angiosystem specific calculation methods such as GE DoseWatch (GEMS, Milwaukee, WI), Siemens CareMonitor (Siemens Healthcare, Erlangen, Germany), Canon Dose Tracking System (Canon Medical Systems, Otawara, Japan) and Philips DoseWise (Philips Healthcare, Amsterdam, Netherlands). In addition, vendor neutral software such as DOSE (QAELUM, Leuven, Belgium) and Em.dose (esprimed SAS, Villejuif, France) exist for this task. These monitoring softwares account for various live information such as tube angulation, energy and amount of radiation at each angulation and location of the patient table to estimate MSD and its location with the maximum reference point air kerma (RPAK). As such, their accuracy depends on the largely unpublished included information but also on the algorithm processing it and how the result is presented. For example, DoseWatch presents the information as a map whereas CareMonitor displays only the maximum value. Already on the market, they provide an easily interpreted real-time estimate of MSD and, commonly, also its location on the patient skin.

2.2.5 Organ dosimetry

Patient organ dosimetry is perhaps most commonly performed with passive solid-state dosimeters, either attached to a patient or more commonly inside a phantom. Passive dosimeters measure the dose by absorbing energy proportional to the amount of radiation. Today, the most common dosimeters in Finland are radiophotoluminescence (RPL) dosimeters (Manninen, 2014), thermoluminescence dosimeters (TLD) (McKeever et al., 1995) and metal oxide semiconductor field effect transistor (MOSFET) dosimeters (Chida et al., 2009).

With TLD, radiation is captured inside a crystal and released as light when heated. TLD crystals are very small and, depending on the material, are suitable for many radiation energies. However, the angular dependency of traditional TLDs is significant (Jin et al., 1992), making them a less ideal option for procedures or examinations with multiple projections. MOSFET dosimeters were originally developed for radiation therapy and have only relatively recently been proven suitable for diagnostic energies (Kaasalainen, 2015).

In RPL dosimeter materials, electrons transferred to the conduction band by ionizing radiation migrate into deep traps. These deep traps are earth or transition metal (i.e., silver) ions doped as impurities into the phosphate material. The proportioned trap can then be photoexcited without the electron being erased back into the conduction band (Riesen and Liu, 2012). As such, RPL dosimeters can be repeatedly read out by photo excitation without fading in the signal per reading. Of these potential methods, RPL dosimetry was chosen to be used in this thesis based on availability and accuracy. RPL dosimetry has good accuracy and repeatability at low doses (20 µGy - 11 mGy) with an average coefficient of variation between 0.5% and 6% (Hsu et al., 2007, 2006; Lee et al., 2009; Manninen et al., 2012; Rah et al., 2009). The energy response of RPLDs is linear between 50 and 125 kVp with a 2.9% mean error (Manninen et al., 2012) and the method's angular dependence is very good up to 30 degrees (Manninen et al., 2012).

Besides measuring, organ doses are also commonly estimated using Monte Carlo calculations (Andreo, 1991). In Monte Carlo methods, each x-ray and their target are simulated with probabilities given for each interaction. One such widely used software is PCXMC (STUK, Helsinki, Finland) (Servomaa and Tapiovaara, 1998).

2.2.6 CT imaging

CT imaging is a topic of recent doctoral dissertations (e.g. Kaasalainen, 2015; Niiniviita, 2017), and due to its minor role in this thesis, only a small glimpse is provided here. As mentioned above, cardiological use of radiation is no longer limited to only IC, but common diagnostic studies such as pre-procedure TAVI CT scan also contribute to patients' total dose. CT imaging is performed using CT scanners with the patient lying down on the scanner table and the X-ray tube and curved detectors rotating around the patient inside a gantry. In a volume scan, the patient table is stationary during imaging, whereas in a helical scan, the patient table moves. Both types of scans can be used for the imaging of longer areas due to sophisticated algorithms calculating the resulting 3D images and sets of 2D images. CT radiation doses are typically described with the CT dose index (CTDIvol) and dose length product (DLP), which is calculated as CTDIvol multiplied by the length of the imaged area.

For heart imaging, CT scans are often performed phased, i.e. ECG gated, to control for and minimize the effect of movement. ECG gating is performed by collecting ECG data during the scan and prospectively triggering the scan at certain phases or retrospectively filtering it using only the suitable phase for reconstruction of the images. The most common phases are arterial and venous phases and their timing depends on the scanned body area. Respiratory movement is typically minimized by performing the scan in a breath hold.

With the ease and speed of scanning, relatively modest price and highly repeatable diagnostics, CT imaging has become prevalent, and its doses have long been considered relatively high (Niiniviita, 2017). This has served as great motivation for dose optimization for both medical physicists and CT manufacturers. The most significant technological advancements in CT imaging have been improvements in iterative calculation for better image quality and dose saving; the speed of scanning, either with improved coverage or a faster scanning area movement for better temporal resolution of repeated dynamic imaging; and spectral or dual energy imaging for the resolution of selected material compositions.

2.3 Big data and data mining

Similarly to CT imaging, big data and data mining are vast topics, and only a glimpse is offered here to illustrate the scope of how they were touched upon in the thesis. In medical practice, as diagnosis and treatment decisions gradually move toward evidence-based medicine (Sackett et al., 1996), data behind the evidence and its analysis and interpretation become more and more important. As such, interest in big data and data mining is growing with a trove of possible applications in healthcare (Beam and Kohane, 2018). One of those methods is machine learning, and one of the applications is optimizing the use of radiation; in particular, the above mentioned difficulty levels can be seen as a suitable application. Machine learning is considered a subset of artificial intelligence. Similarly, deep learning is considered a subset of machine learning.

In general, machine learning algorithms focus on handling big data in an objective, reliable and repeatable way, offering insight into predicting how the data will behave in the future. Machine learning algorithms require training, during which they are provided sufficient data and means to classify it with a loss function. By splitting the data repeatedly into random training and testing data sets, the machine learns to optimize the classification by minimizing the loss function, simultaneously assessing its own performance. Applying statistical significance to machine learning is a complex topic (Drummond and Japkowicz, 2010) and is out of the scope for this thesis. Machine learning algorithms are very dependent on the representativeness of the training data.

An example of a suitable machine learning model for dose prediction with difficulty levels is support vector regression (SVR), a supervised machine learning model that predicts continuous output values (i.e., real numbers) by minimizing a pre-defined loss function. Due to convention, machine learning algorithms refer to included parameters as features, and in appropriate parts this convention is also applied in this thesis.

3 Aims

The main aim of this thesis is to answer the need to evaluate doses and minimize risks related to the use of radiation in contemporary cardiological procedures, with an emphasis on newer or more complex procedures such as TAVI and PCI. In the Publications, this was done by a thorough investigation of patient KAP in Publications I, II and IV and skin doses in Publication III. The main questions were:

- What is the current level and variation of use of radiation in cardiology in Finland and in Europe?
    - What is the contemporary level of use of radiation in cardiology in Finland and Europe?
    - How high is the KAP variation and what demographic and clinical factors predict KAP?
- Is patient skin damage possible in contemporary cardiac procedures?
    - If so, what kinds of alert levels for possible skin damage should be set?
    - How accurate are the available automatic skin dose estimating tools GE DoseWatch and Siemens CareMonitor?
- At what level are heart organ doses in TAVI procedures and the prerequisite CT scans in Turku University Hospital?

4 Materials and Methods

4.1 Patient KAP doses

4.1.1 Finnish and European DRLs

In Publication I, data from five university hospitals and two central hospitals in Finland were analyzed to explore the contemporary use of radiation in cardiological procedures. Namely, the Turku, Helsinki, Tampere, Kuopio and Oulu University Hospitals and Joensuu, Jyväskylä and Vaasa Central Hospitals participated in the study. These hospitals were coded as UH1-5 (university hospital) and CH1-3 (central hospitals. The data were collected between 2014 and 2016 for both scientific research purposes and to provide the STUK with the necessary data for new DRLs. As such, the study was performed in close collaboration with the STUK. At the time of data collection, electrophysiological and TAVI procedures were performed only in the university hospitals. Since then, some central hospitals have also begun performing them. The participating hospitals were chosen based on the amount of procedures performed and the willingness to participate. Not all hospitals were able to provide data on all requested parameters, such as fluoroscopy or cine KAP or FT or total imaging time. Ethical permission was received (T72/2016), and the request for patient consent was waived due to the observational and anonymized setting.

The initial distribution of collected procedures and difficulty levels is shown in Table 1, which was formed based on input from cardiologists and other experts from multiple hospitals.

Table 1. Initial distribution of proposed bolded procedure types and difficulty levels.

Coronary procedures	**Pacemaker Implantations**	**Electrophysiological procedures**	**TAVI procedures**
CA	Single chamber PI	Atrial fibrillation	Transapical
Elective PCI	Dual chamber PI	AVNRT	Transfemoral
ad hoc PCI	CRT	Atrial flutter	Transaortic

The gathered data contained a portion collected with excel sheets, which contained descriptive parameters presented in Table 2 and a portion collected from radiation dose registries, which contained varying amounts of parameters but was mainly limited to total KAP and FT. In total, data from 21 278 procedures were collected in Publication I.

Table 2. Collected descriptive parameters in the data with excel sheets.

Patient age	Patient weight
Patient height	Patient gender
Fluoroscopy time	Total imaging time
Fluoroscopy dose	Cine dose
Amount of Cine series	Air kerma

With the excel sheets, a questionnaire was sent to outline the use of personnel shielding, typically used projections and collimation, and KAP meter errors as reported by regular maintenance. The KAP meter errors were accounted for in all publications.

In both Publications I and II, the DRLs were calculated as third-quartile values of the hospitals' medians for the quantity in question, which is in line with the ICRP recommendations (ICRP, 2017) and methodology of the Finnish authority (STUK) for the new DRLs (STUK, 2016). In the EU-wide data collection (Publication II), Finnish data were combined with data from 11 other European countries (Belgium, Croatia, Czech Republic, France, Greece, Ireland, Poland, Serbia, Spain, Sweden and Switzerland). In total, the data in Publication II were gathered from 14922 procedures. The descriptive parameters were the same as for Publications I and II. In addition to the above analysis methods, an uncertainty analysis was performed to account for the varying KAP meter errors and the effect of each country's median value on the European DRL. The former was performed using available correction factors or nationally mandated maximum errors, whereas the latter was calculated separately for each procedure.

4.1.2 Statistical and machine learning analyses

In Publications I and II, DRLs were calculated from the third quartiles of the hospitals' median values in accordance with the ICRP's 135 recommendations (ICRP, 2017). Mainly, the amount of data was also in accordance with the recommendations. To study parameters predicting KAP in Publication I, for the cases where complete data were available, Spearman correlation coefficients with

95% confidence intervals (95% CI) calculated using Fisher's z transformation were used in the four procedure categories of coronary procedures, pacemaker implantations, electrophysiological procedures and TAVIs. For binary variables (patient gender, previous bypass surgery and cardiologist fellow or trainee), a Kruskal-Wallis test was performed to test the differences between the groups. An AHA classification was treated as an ordinal variable ranging from low to high difficulty and from a low to high radiation dose.

Two-tailed tests of significance (95% CI) were performed to assess the dose level differences between hospitals and how they deviated from the national median. Due to the assumption of normality, the dose data were transformed with natural logarithm and normality was checked with histograms. Even after the transformation, several procedures performed in UH2 (CA, PCI and PI) were conspicuous as having anomalously high numbers of low doses, but generally, the data were deemed sufficiently normal. Dose level differences between different procedures or between hospitals were tested with t-tests for independent samples.

The statistical analysis methods in Publication I were selected based on the amount of obtained data and their variance. Statistical power was not calculated before data collection. Statistical analyses were performed by an experienced statistician using SAS System for Windows, Version 9.4 (SAS Institute Inc., Cary, NC). No data imputation was carried out and only some obvious typos were removed from the data.

In Publication IV, features predicting patient KAP in CA and PCI procedures were studied with the retrospectively collected cohort data (n=2179) from Turku University Hospital's electronic dose and health records using GE DoseWatch (GEMS, Milwaukee, USA), the PCI procedure registry (BCB Mecical, Turku, Finland) and Uranus (CGI, Montreal, Canada). The timeframe was from January 2016 to December 2017 and data were collected using a single Siemens Artis Zee Ceiling (Siemens Healthcare, Erlangen, Germany) with the dose data corrected with the latest dosimeter accuracy report. The only inclusion criterion was availability of information on both the DoseWatch and PCI procedure registry of each procedure. The feature selection methodology consisted of nine statistical filter-based methods, which are independent of the regression model and, as such, are less prone to overfitting (Guyon and Elissee, 2003), and an SVR supervised machine learning model. The nine filter-based methods were F-value regression (FREG), mutual information regression (MIR), SURF (SURF), SURFstar (SURFS), MultiSURF (MSURF), MultiSURFstar (MSURFS), Pearson correlation coefficient (PEAR), Spearman correlation coefficient (SPEA) and ReliefF (RELF).

In order to not discard many of the parameters, missing data were imputed with the median value when not directly implicit in the data (such as in the case of yes-or-no questions). The data were first randomly split into training data (80%) and testing data (20%). Categorical features in the data were one-hot encoded, and all features were scaled logarithmically to optimize the performance of the regression model. Pair-wise Spearman correlations between the features were checked.

The included 59 patient demographic and clinical features are shown in Tables 3 and 4. Of the procedures, FN1AC denotes coronary angiography (CA) and FN2BA PCI with stent. Of the diagnoses, I35.0 denotes non-rheumatic aortic valve stenosis, I20.81 other angina pectoris (AP) with constricted coronary artery (stenosis), I21.01 ST elevation myocardial infarction (STEMI) involving the left main coronary artery, I21.11 STEMI involving the right coronary artery and I21.41 non-ST elevation myocardial infarction (NSTEMI) with stenosis. Of the indications, UAP denotes unstable angina pectoris. Previous CABG refers to a previous coronary artery bypass grafting. Body surface area was calculated with the Du Bois formula (DuBois, 1916) and body mass index (BMI) using the standard formula. The number of procedures denotes the number of billed procedures performed. Pre-stenosis refers to stenosis before PCI and post-stenosis to stenosis after PCI. Chronic total occlusion (CTO) refers to long-occluded coronaries and LM unprotected to the unprotected left main coronary in the procedure. The AHA score refers to AHA/ACC lesion classification. Additional stenting 1 refers to the use of 2 stents and additional stenting over 1 to the use of more than two stents.

Table 3. Numerical features assessed in Publication IV.

Feature	Unit	Mean	SD	Min	Max	% missing
Age	years	69.8	11.7	33	97	0.0
Weight	kg	82.2	16.8	44	176	0.0
Height	cm	172	9.3	142.5	194	27.1
BSA[a]	m^2	1.9	0.2	1.4	2.8	27.1
BMI[b]	kg/m^2	28.2	4.9	18.3	50.0	27.1
Stent dimension	mm	3.3	0.6	2.2	5.6	74.9
Ball dimension	mm	3.2	0.8	1.0	5.2	84.1

[a] Body surface area
[b] Body mass index

Table 4. Categorical features assessed in Publication IV.

Feature	Categories	% missing
Gender	male/female	0.0
Procedure	FN1AC[a] or FN2BA[b]	0.0
Indication	PCI in STEMI, Flap failure, NSTEMI, Diagnostic, UAP, Heart failure, STEMI other, Stable AP or Arrhythmia settlement	19.9
Coronary segment	LADa, LADb, LADc, LCXa, LCXb, LCXc, LD1, LM, LOM1, RCAa, RCAb, RCAc, RPD	35.7
Diagnosis	I35.0[c], I20.81[d], I21.01[e], I21.11[f] or I21.41[g]	0.0
Multi-vessel disease	yes/no	0.0
Previous CABG[h]	yes/no	0.0
AHA/ACC score[i]	A, B1, B2 or C	50.2
CTO[j]	yes/no	0.0
Restenosis	yes/no	0.0
LM unprotected	yes/no	0.0
Pre-stenosis	60%, 85% or 100%	51.7
Post-stenosis	0%, 25%, 60%, 85% or 100%	51.7
Additional stenting	1 or over 1	0.0
Number of procedures	1, 2 or 3	0.0

[a] CA
[b] PCI with stent
[c] Nonrheumatic aortic (valve) stenosis
[d] Angina pectoris
[e] ST elevation myocardial infarction (STEMI) involving left main coronary artery
[f] STEMI involving right coronary artery
[g] Myocardial infarction without ST elevation
[h] Coronary artery bypass grafting
[i] American Heart Association/American College of Cardiology
[j] Chronic total occlusion

After preprocessing the data, the nine filter-based methods were used to obtain rankings for the best features, which were then used as inputs for the SVR. The number of features varied from 5 to 40 to assess each methods' accuracy. The mean square error (MSE) was selected as the loss function that was minimized. A margin of tolerance " was also determined and no penalty was associated in the loss function with points predicted within a distance " from the actual value. In addition, since SVR does a linear prediction on the data, a radial basis function (RBF) kernel was used to transform the parameters into hyperparameters. In Publication IV, radial basis function (RBF) kernel was used. The SVR model was implemented using scikit-learn (v0.20.3) in Python (3.5.3) (Pedregosa et al., 2011).

Before initiating the SVR, various parameter combinations were studied using grid search by iterating over all the possible combinations of the given grid. The performance of each hyperparameter combination was evaluated using 5-fold cross-validation on the training data and calculating a validation MSE for each fold. The mean error over all 5 folds was then selected as the performance metric of the given hyperparameter combination and the process was repeated for the next set of hyperparameters. Once all hyperparameter combinations had been evaluated, the lowest mean error was selected as the optimal set of hyperparameters for the given n features. The SVR model was then refitted on the whole training set using these hyperparameters. Finally, the fitted model was used to make predictions on the test set with the same n features, and the test MSE was calculated based on the test predictions as the final performance metric.

An illustration of the data processing pipeline is shown in Figure 7. The algorithm was repeated 100 times using a new randomization seed in every iteration, which was found to ensure the stability and repeatability of the results.

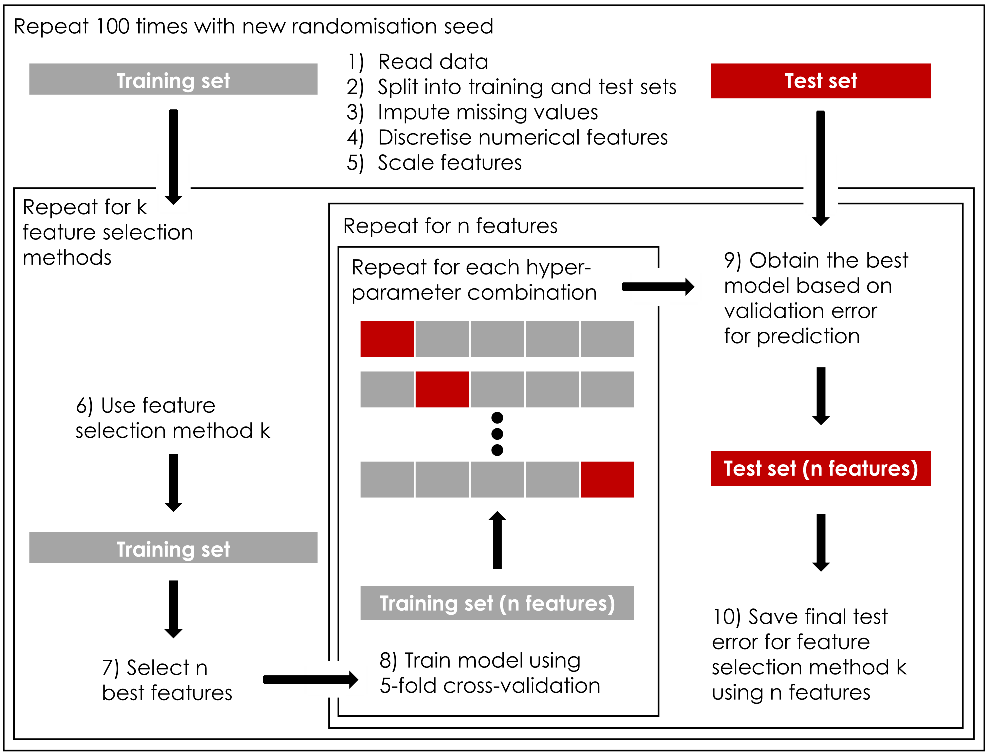

Figure 7. Overview of data processing pipeline in Publication IV: 1) The data was read into a dataframe; 2) split into training and test sets; 3) imputed based on the training set; 4) the features were log-scaled; 5) feature selection method (k = 1-9) was used on the training set; 6) the highest-ranking features (n = 5, 10,..., 40) were obtained; 7) the n features from the method k were used to train a support vector regression (SVR) model using hyperparameter grid search with inner 5-fold cross-validation; 8) the SVR model was refit on the whole training set using the combination of hyperparameters based on the lowest cross-validation mean squared error (MSE); 9) the fitted SVR model was used to predict the radiation dose in the test set with the same n features and the test MSE was saved. Steps 1-9) were repeated 100 times with a new randomisation seed.

4.2 Patient skin dose measurements

Concurrently with the excel sheet collection of KAP values, Gafchromic films were irradiated under patients in seven of the hospitals. The films' usage during the procedures, storage and transportation were carefully instructed. After irradiation, the films were sent to the STUK for calibration and scanning. They were calibrated following the methodology presented by Alnawaf et al. (Alnawaf et al., 2010). The calibration included the following steps:

- Estimation of the most suitable radiation quality based on the most-used radiation energies

- Irradiation of pieces of film with suitable doses with a frequently calibrated and measured X-ray device
- Scan of the calibration data with a dedicated scanner in reflective mode
- Five measurements of the darkening and background each
- Fitting of the data

The participating hospitals were shown how to handle the films with care, store them inside a black bag and a cardboard box and position them correctly under the patient. After irradiation, these boxes were sent to the STUK, where they were analyzed with the Epson Expression 1600 Pro scanner. Initially, ten films were distributed to each hospital, but more data were gathered in 2018 at the Turku and Kuopio University Hospitals, and a new calibration was performed. The newer films were scanned with the Epson Expression 12000XL scanner.

In the initial calibration, dose amounts 0.1, 0.5, 1.0, 3.0 and 5.0 Gy were used with radiation quality defined by the International Electrotechnical Commission's (IEC) RQR5 (Commission et al., 1994), a typical radiation quality for diagnostic use of radiation. In the newer calibration, dose amounts of 0.1, 0.25, 0.5, 1.0, 1.5, 2.0 and 3.0 Gy were used. The two calibration fits are shown in Figure 8, and examples of irradiated films are shown in Figure 9. The two calibrations were compared with t-testing ($P<0.05$) after logarithmic transformation of the data.

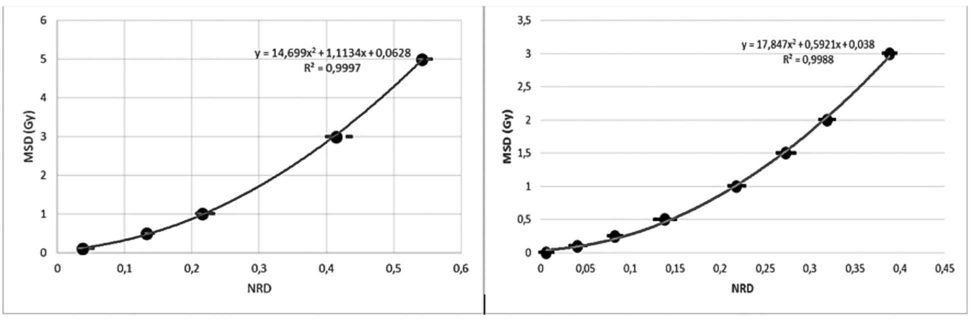

Figure 8. Gafchromic film calibration as maximum skin dose (MSD) vs. net reflective density (NRD). The horizontal lines denote the measurement errors. Left: earlier calibration from 2016. Right: newer calibration from 2018. Published in Publication III.

Film darkening due to irradiation was measured using ImageJ (Rasband, 2016). Film absorbance or net reflective density was calculated from background and maximum darkening as

$$A = \log (I_0=I), \quad (1)$$

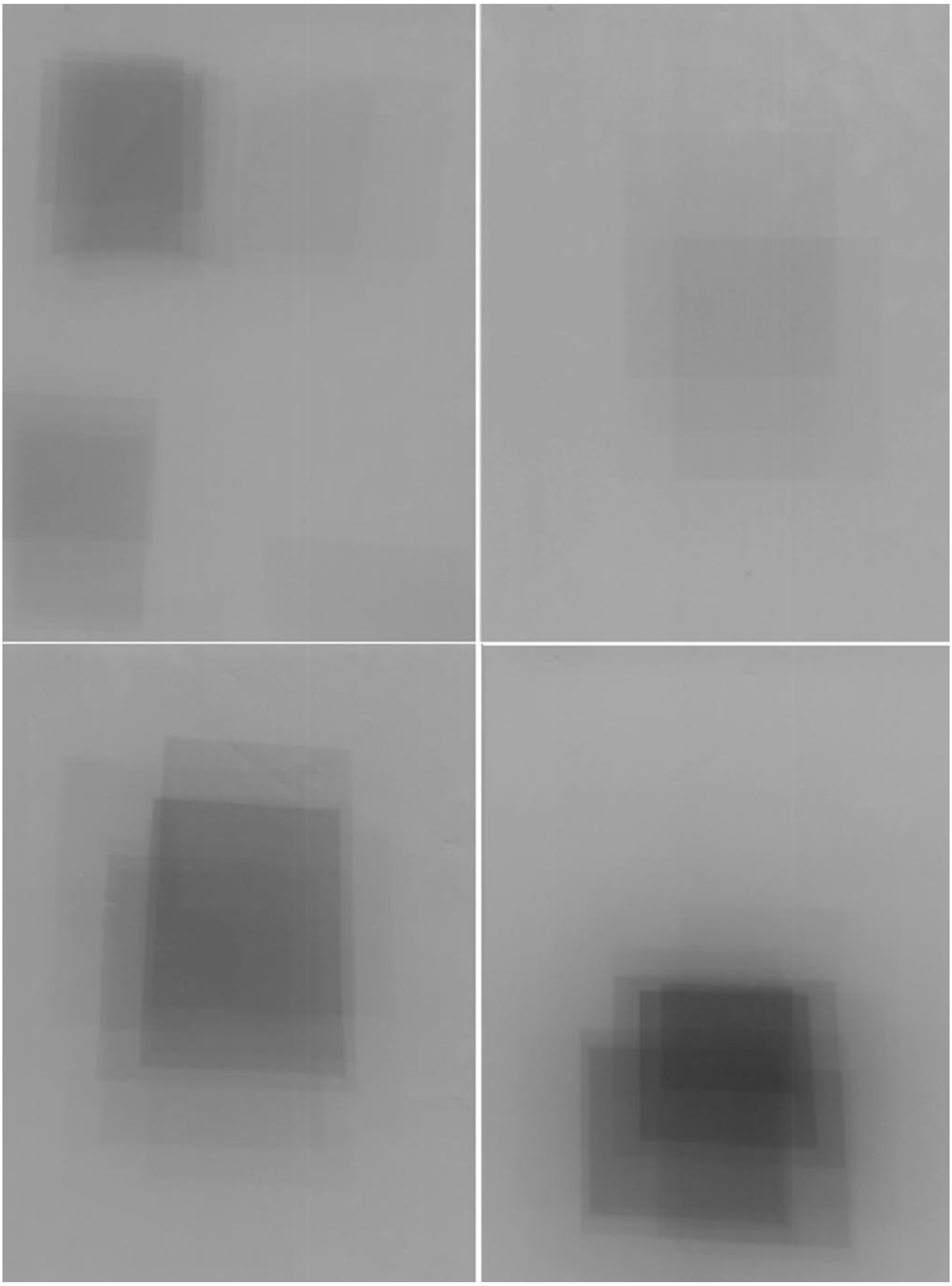

Figure 9. Examples of irradiated films. Up left: PCI with MSD 377.3 mGy, KAP 53.9 Gy·cm^2 and air kerma 1277 mGy. Up right: PI with MSD 125.3 mGy, KAP 1.1 Gy·cm^2 and air kerma 127 mGy. Down left: Electrophysiological procedure with MSD 415.4 mGy, KAP 71.5 Gy·cm^2 and air kerma 893 mGy. Down right: TAVI with MSD 3.20 Gy, KAP 120 Gy·cm^2 and air kerma 2104 mGy. Published in Publication III.

where I_0 is the measured background intensity on the same film and I the measured mean intensity of 1 cm^2 of maximum intensity. In the calibration, film absorbance was then fitted binomially to the irradiated dose and the resulting fit was used to determine the corresponding maximum skin dose of patients (Alnawaf et al., 2010).

Measured maximum skin doses were used to estimate KAP and air kerma alert levels if the resulting fit of MSD vs. KAP or air kerma was reasonable and had a sufficient amount of data points above 2 Gy MSD. In addition, Spearman correlations of MSD with other parameters (Table 2) were calculated, and MSDs were compared to maximum local RPAK values obtained from GE DoseWatch and Siemens CareMonitor.

Lastly, an analysis of measurement errors was carried out following the methodology detailed by Farah et al. (Farah et al., 2015) and an experienced statistician was consulted about its most complex portions. The analysis focused on scanner, film-to-film, calibration fit and film dose rate uncertainties. Scanner uncertainty was determined by extensively testing the scanner daily for two months for long-term homogeneity testing and hourly during measurement days for short-term homogeneity testing. Film-to-film uncertainty was measured using the background values of films from the same batch. Calibration fit uncertainty was determined from the slope of the fit at 1.75-2.25 Gy for both the initial and the newer calibrations. Film dose rate uncertainty was checked at 0.5, 0.28 and 0.14 mGy/s. The angiodevices' KAP-meter display accuracies provided by regular maintenance were also accounted for, and all collected KAP-values were corrected accordingly.

4.3 Heart organ dose measurements

To measure the heart doses of a TAVI procedure and a pre-procedure CT-scan, RPL (GD-352M, 2019) dosimeters with a tin filter and an automatic reader (Dose Ace FGD-1000, Asahi Techno Glass Corporation, Chiba, Japan, 2016) were used to measure the absorbed doses. The measurements were carried out with brand new dosimeters. The reader's calibration was performed with calibration dosimeters (GDS-352A) before the measurements as well as with an internal daily calibration check before reading the results. The calibration dosimeter's irradiation dose was 6 mGy free in air with Cs-137.

To carry out the measurements, an anthropomorphic phantom (ATOM male phantom model 701, CIRS, Norfolk, Virginia, USA) was implanted with RPL dosimeters to measure radiation absorbed in the heart. In total, 20 dosimeters were emptied. Two dosimeters were used as references, nine were used in the CT scan and nine in the TAVI procedure. In both the CT scan and the TAVI procedure, the dosimeters were placed in three slices in the location of the heart. An example of dosimeter positioning is shown in Figure 10; the Figure 10 also shows the used Atom phantom positioned on the GE Discovery MI PET / CT scanner with 64 slices (GEMS, Milwaukee, WI), which was used for the CT measurements at Turku University Hospital's PET Centre.

Figure 10. Example images of RPL dosimeter positioning inside the ATOM anthropomorphic phantom (left), phantom positioning on GE Discovery PET / CT table (middle) and phantom positioning on Siemens Artis Zeego table (right).

The CT scan consisted of a diastolic ECG (R-peak delay 60%), a breathgated heart scan and a body scan optimized for TAVI. In addition, anteroposterior (AP) and lateral (LAT) scout scans and 10 preparation series for gating at the bifurcation level were included in the CT scan. The CT protocols are presented in Table 5.

Table 5. Relevant heart CT protocol parameters in clinical use in Turku university hospital PET centre GE Discovery MI (GEMS, Milwaukee, WI).

	Gated heart scan	**Body scan for TAVI**
Scan type	Volume	Helical
kV	120	120
mAs	470	540
Noise index	NA	15.0
Slice thickness	0.625 mm	0.625 mm
Pitch	NA	1.375
Iterative reconstruction	ASiR 40%	ASiR 40%
$CTDI_{vol}$	29.94 mGy	10.95 mGy
Gating	R-peak delay 60%	None

After changing the dosimeters, the rest of the measurements were carried out with the Siemens Artis Zeego (Siemens Healthcare, Erlangen, Germany) at the Turku

University surgical ward, the angiosystem most used for TAVI procedures at Turku University Hospital. The TAVI procedure was estimated from the collected parameters for Publication 1, protocol data from the used angiosystem for kV, mAs and detector doses. In addition, one year's data from the GE DoseWatch (GEMS, Milwaukee, WI) were gathered to estimate how much FL and cine is used in each projection. The phantom was positioned so that the dosimeters were irradiated for all of the procedure. The positioning of the phantom is shown in Figure 10. The 2016 Finnish DRL (STUK, 2016) was used as the total KAP of the procedure. The parameters for the TAVI procedure are presented in Table 6. Both the CT and TAVI protocols are in clinical use.

Table 6. Relevant TAVI protocol and procedure parameters as estimated from the collected parameters for Publication 1 and local data from Turku university hospital's Siemens Artis Zeego and GE DoseWatch (GEMS, Milwaukee, WI).

Protocol fluoroscopy kV	70
Protocol Cine kV	81
Protocol fluoroscopy detector dose	45 nGy/p
Protocol Cine detector dose	0.240 μGy/fr
FOV	25 cm
SID	110 cm
SOD	70 cm
OID	15 cm
Total KAP	90 Gy·cm^2
Most used projection	PA
Second most used projection	LAO 10
Third most used projection	RAO 10
Fluoroscopy dose at most used projection	24.2 Gy·cm^2
Cine dose at most used projection	21.6 Gy·cm^2
Fluoroscopy dose at second most used projection	11.7 Gy·cm^2
Cine dose at second most used projection	9.4 Gy·cm^2
Fluoroscopy dose at third most used projection	8.3 Gy·cm^2
Cine dose at third most used projection	14.1 Gy·cm^2

Before the reading, the dosimeters were pre-heated as recommended by Manninen et al. (Manninen et al., 2012). The dosimeters were read five times and their average value was used to represent the heart dose. As the system used by Manninen et al. (Manninen et al., 2012) was considered to be identical but older, determination of uncertainty of the measurements was limited to the repeatability check of the background doses and dose reading uncertainty.

5 Results

5.1 Patient KAP doses

5.1.1 Finnish and European DRLs

Both Finnish and European data collections became relatively weighted toward retrospective data. From the perspective of forming DRLs, this was not a problem, but this posed a challenge for further analysis. The amount of data for the descriptive parameters is shown in Table 7.

Table 7. Amount of data and descriptive statistics for descriptive parameters in Publication I.

	Amount of data	**Average**	**Range**
Date of procedure	1001		2014 - 2015
Patient age	916	66.3	19 - 98
Gender	917	64.4% male	
Weight (kg)	994	82.0	38 - 164
Height (cm)	993	171.2	65 - 198
Previous bypass surgery (yes/no)	999	6.9% yes	
AHA/ACC classification	198	B1	
Fluoroscopy DAP ($Gy{\cdot}cm^2$)	716	12.3	0 - 165.0
Cine DAP ($Gy{\cdot}cm^2$)	662	26.9	0 - 794.4
Number of acquisitions	758	14.0	0 - 108
Air kerma (mGy)	938	605.3	1 - 11162.5

Initially, dose levels of all the proposed difficulty levels were checked. As a result of the t-tests, differences between elective and ad hoc PCI and single and dual chamber pacemaker implantations were not statistically significant and the difficulty levels were combined. As for TAVI difficulty levels, the transapical access route was so overwhelmingly popular that all difficulty levels had to be combined. In addition, of the electrophysiological procedures, AF had significantly higher doses than AVNRT or atrial flutter. After discussing the matter, the concept of difficulty levels was dropped from the publication. The final procedure categorization is shown in Table 8.

Table 8. Final procedure categorization in Publication I.

Coronary procedures	Pacemaker Implantations	Electrophysiological procedures	TAVI procedures
CA	PI	AVNRT	TAVI
PCI	CRT	Atrial flutter	
		Atrial fibrillation	

In Figure 11, the dose levels of various hospitals in Finland are shown. As mentioned in Chapter 4.1, DRLs were calculated as the third quartiles from hospitals' medians for each procedure. Because of the low amount of data, some results shown in Figure 11 were excluded from DRL calculations. Namely, CH 1 was excluded from the PI DRL and UH4 was excluded from the PCI DRL. Not all the procedures were given a DRL. Namely, for CRT, AVNRT and atrial flutter procedures, the number of hospitals that provided sufficient data was too low to calculate the DRL in accordance with the ICRP 103 (ICRP, 2007), and tentative KAP values were used instead.

Published KAP DRLs and FT third quartiles calculated similarly to DRLs are shown in Tables 9 and 10. The approach with FT was chosen due to its complex relation to KAP (Chapter 2.2.) and to recommendations by ICRP (ICRP, 2017). The tables also include comparable data from other published results in the literature.

In addition, Figure 12 shows how TAVI doses decreased in Finland during the data collection period. Although the reported Spearman correlation in Publication I was not statistically significant (-0.082, P=0.151), it supports the notion of a learning curve.

With good statistics in the t-tests, many hospitals deviated significantly from the total data median in CA procedures. Likewise, UH1 deviated significantly from the total data median in TAVI procedures.

Dose variation in the countries that participated in the study published in Publication II is shown in Figure 13, which illustrates that dose variation is most pronounced in high-dose studies like PCI and TAVI and is even greater at the international scale than in Finland.

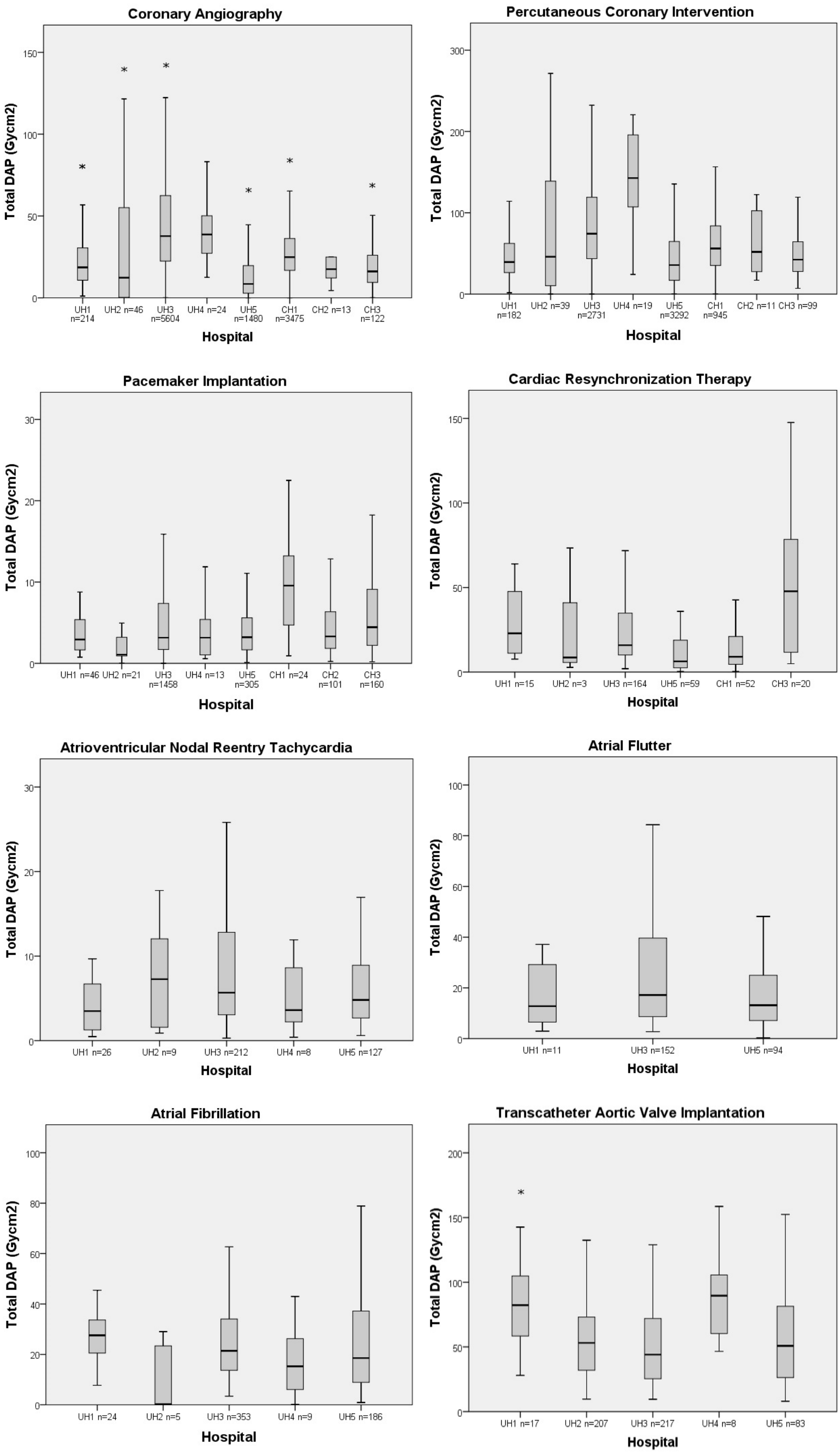

Figure 11. Cardiological patient KAP doses in Finland as published in Publication I.

Table 9. Published and relevant comparison KAP (Gy·cm2) DRLs in Publication I.

Publication / procedure	CA	PCI	PI	CRT	AVNRT	Atrial flutter	AF	TAVI
Publication I	30	75	3.5	22[b]	6[b]	16[b]	25	90
Finnish DRL 2006[c]	60	100						
Sentinel, EU, 2008[d]	45	85						
RAD-IR, USA, 2003[e]	83	193						
Switzerland DRL 2018[f]	50	100	5		EF 20	RFA 30		100
Ireland DRL 2008[g]	46.5	106.5	16.9					
Croatia DRL 2009[h]	32							
Bulgaria DRL 2012[i]	40							
Greece 75th percentiles 2013[j]	53	129	36			RFA 146		
Pantos et al averages 2009[k]	39.9	78.3			EF 14.5	RFA 54.6		
Norway DRL 2010[l]	21							
Australia DRL 2014[m]	58.6	129						
2nd RA' ACT France DRL 2017[n]	26	60						
UK DRL 2009[o]	29							

[a] (STUK, 2016)
[b] Tentative DRL calculated as DRLs.
[c] (STUK, 2005)
[d] (Padovani et al., 2008)
[e] (Miller et al., 2003a,b, 2012)
[f] (BAG, 2018)
[g] (D'Helft et al., 2008)
[h] (Brnic et al., 2009)
[i] (Zotova et al., 2012)
[j] (Simantirakis et al., 2013)
[k] (Pantos et al., 2009)
[l] (Statens strålevern, 2010)
[m] (Crowhurst et al., 2014)
[n] (Georges et al., 2016)
[o] (Hart et al., 2009)

Table 10. Published and relevant comparison fluoroscopy times (min) in Publication I.

Publication / procedure	CA	PCI	PI	CRT	AVNRT	Atrial flutter	AF	TAVI
Publication I[a]	6.0	18.4	6.7	20.5	13.3	23.1	14.0	21.5
Finnish DRL 2006[b]	8	20						
Sentinel, EU, 2008[c]	6.5	15.5						
RAD-IR, USA, 2003[d]	5.4	18.5						
Switzerland DRL 2018[e]	8	20	5		EF 10	RFA 9		30
Ireland averages 2008[f]	4.3	14.5	6.6					
Croatia DRL 2009[g]	6.6							
Bulgaria DRL 2012[h]	5.1							
Pantos et al averages 2009[i]	4.7	15			EF 9	RFA 45.8		
2nd RA' ACT France DRL 2017[j]	4	11						
UK DRL 2009[k]	4.5	13	8.2					

[a] 3rd quartile values calculated similarly to DRLs.
[b] (STUK, 2005)
[c] (Padovani et al., 2008)
[d] (Miller et al., 2003a,b, 2012)
[e] (BAG, 2018)
f (D'Helft et al., 2008)
[g] (Brnic et al., 2009)
[h] (Zotova et al., 2012)
[i] (Pantos et al., 2009)
j (Georges et al., 2016)
[k] (Hart et al., 2009)

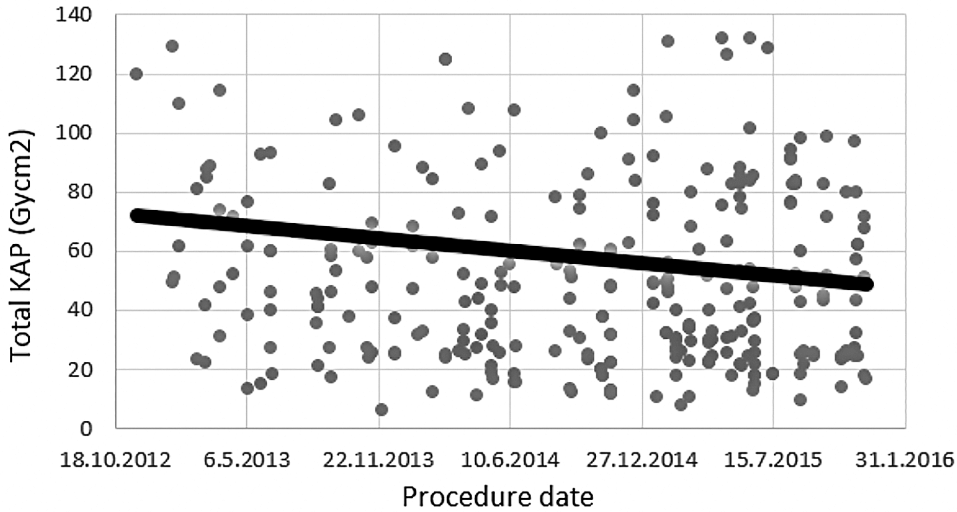

Figure 12. How TAVI doses have changed in time in Finland as published in Publication I.

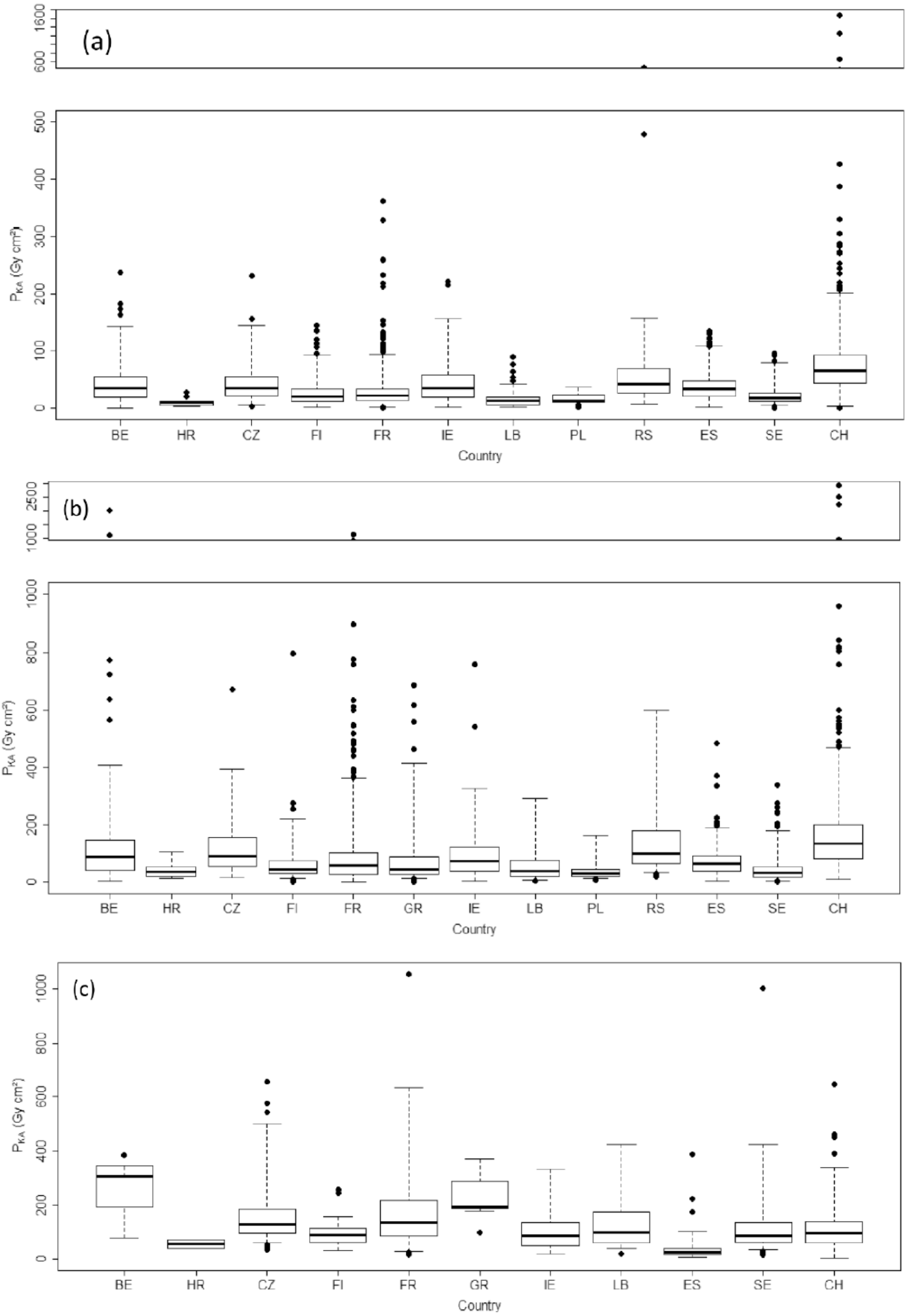

Figure 13. Distribution of total PKA (KAP) values for each country. The data are for CA (a), PCI (b), TAVI (c), PI (d) and EF (e) procedures as published in Publication II.

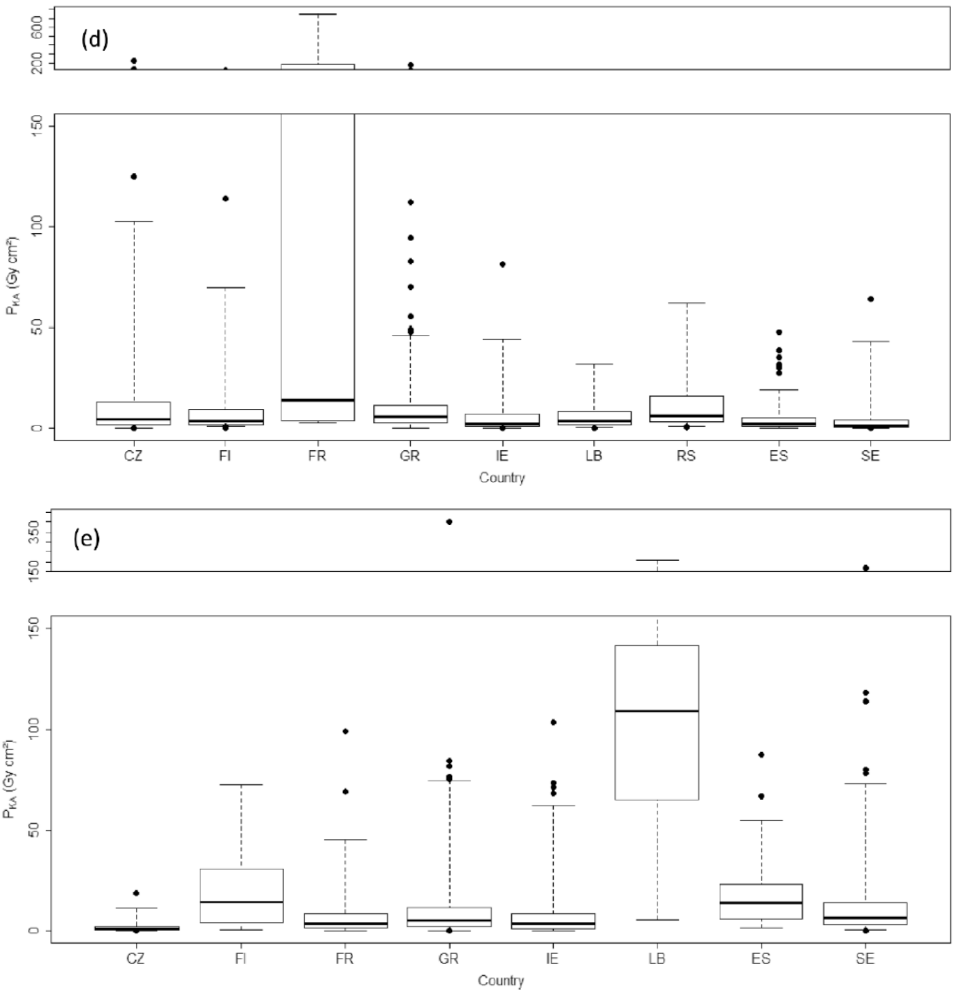

Figure 13. Distribution of total PKA (KAP) values for each country. The data are for CA (a), PCI (b), TAVI (c), PI (d) and EF (e) procedures as published in Publication II (continued).

5.1.2 Features and parameters predicting KAP dose

According to the calculated Spearman correlations, the statistically significant parameters for the total radiation dose in Publication I, in order of correlation, were the amount of cine, FT, patient weight, AHA classification, patient height, angiosystem age and patient age. FT, as mentioned above, had a varying correlation depending on how much cine was generally taken in the procedures. This was especially true for all high-dose procedures, in which the amount of cine correlated strongly with total KAP. For TAVI procedures, weight was the most descriptive of the above factors. Low correlations of AHA score in CA procedures and angiosystem age in all procedures and negative correlations of patient age in PI procedures were noteworthy.

In the Kruskal-Wallis test, male gender was an influential and significant factor for total dose in all procedure types (χ_2 = 68.56 with p<0.001 for coronary procedures; χ_2 = 13.33 with p<0.001 for pacemaker implantations, χ_2 = 4.72 with p<0.05 for electrophysiological procedures and χ_2 = 7.08 with p<0.01 for TAVI). In addition, a patient's previous bypass surgery had a significant but minor effect on dose in coronary procedures (χ_2 = 6.81 with p<0.01). A cardiologist fellow or trainee performing the procedure had no significant effect on the total radiation dose. This was the case for all procedure types.

As demonstrated in Publication IV, features predicting the use of radiation in coronary procedures are shown in Figure 14. Pair-wise Spearman correlations occurred mainly with demographic features and between some diagnoses and indications, as shown in Figure 15.

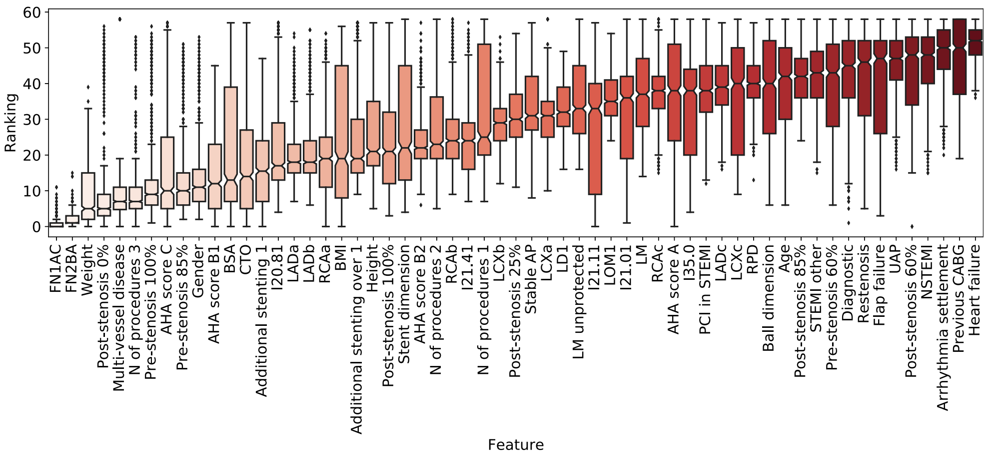

Figure 14. Boxplot showing the feature rankings (range 0-58 from best to worst) from 9 different filter-based feature selection methods (9 methods x 100 repetitions = 900 rankings per feature) in estimating the treatment radiation dose. The features are ordered by their median value based on the rankings. Boxes show the interquartile ranges (IQR) with median values (notch) and whiskers show 1.5 interquartile ranges from the lower and upper quartiles. Outliers are plotted as individual points beyond the ends of the whiskers.

The ten highest-ranking features organized by their aggregate median values were: 1) FN1AC, 2) FN2BA, 3) weight, 4) Post-stenosis 0%, 5) multi-vessel disease, 6) N of procedures 3, 7) pre-stenosis 100%, 8) AHA score C, 9) prestenosis 85% and 10) gender. The first two emphasize the well-established division between CA and PCI, as noted above. Patient weight is a traditional radiation dose predictor and its high rank was also expected.

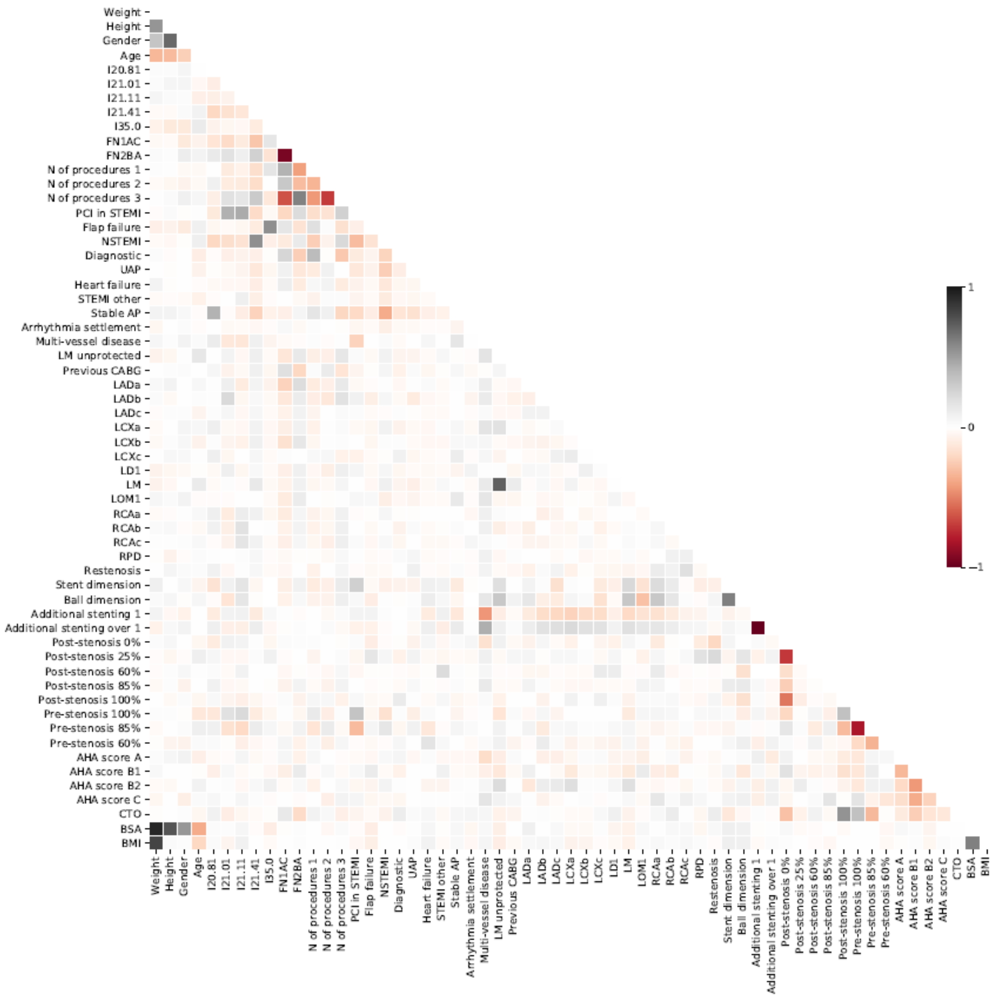

Figure 15. Diagonal correlation matrix showing the pairwise Spearman's correlation coefficients between different features.

Post-stenosis 0% is associated with higher KAP (mean 36.7 Gy·cm^2 compared to mean 28.0 Gy·cm^2 for the whole data set) and was ranked fourth. This association may be due to the required finesse and subsequent imaging to achieve said result. Multi-vessel disease and the high number of performed procedures (3) ranked fifth and sixth, respectively, and they are associated with higher radiation doses as they directly increase the extent and urgency of the procedure. A high number of procedures, however, is strongly correlated with performing PCI. Pre-stenosis 100%, AHA score C and pre-stenosis 85% were ranked seventh, eighth and ninth, respectively. They all imply difficult procedure with high pre-stenosis and tortuous or degenerated vein grafts.

Patient gender was ranked tenth, with men on average induced to 32.5 Gy·cm^2 compared to 18.8 Gy·cm^2 among women. This difference is partly attributable to cross-correlations with patient weight, additional stenting over 1, multi-vessel disease, number of procedures 3 and PCI. All of these point to men in Finland seeking treatment at a later stage of disease, and, compared to women, more must be done to treat them.

AHA score B1 ranked 11th, but B2 and A ranked significantly lower. The AHA score accounts for lesion location, bifurcation, size and shape and coronary tortuosity and angulation. These factors describe PCI complexity in terms of outcome and the result indicates that its applicability to procedure difficulty in terms of use of radiation is not straightforward.

BSA ranked 12th and was most likely affected by its high correlation to weight. CTO ranked 13th, which is lower than expected, and the result was likely affected by the low amount of CTOs (32) and huge dose variations among them (mean dose 69.4 Gy·cm^2 and standard deviation 56.3 Gy·cm^2). Additional stenting ranked 14th and 20th for one and more than one, respectively. Additional stenting implies difficult stent placement and that additional imaging is needed to place further stents.

Results from the prediction performance analysis are shown in Figure 16. They indicated differences in suitability for dose prediction for the methods, as well as clear dependence on the number of included features. The best performing methods were FREG, MIR, PEAR, RELF and SPEA and 30 features was interpreted as a suitable number for the methods to perform optimally.

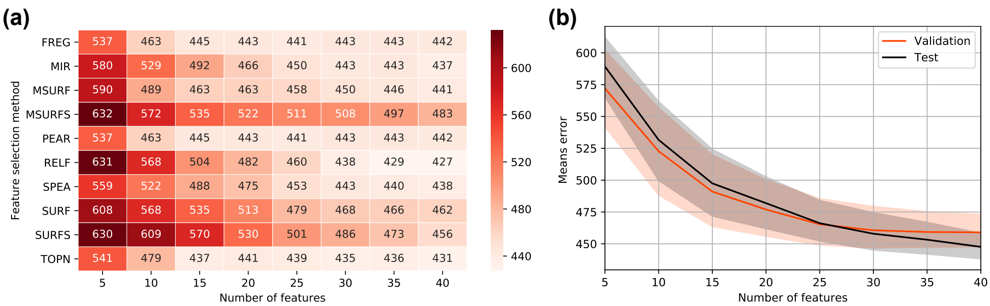

Figure 16. (a) Heatmap showing the mean test errors from support vector regression (SVR) model in estimating the treatment radiation dose. The values show the mean test error from 100 repetitions using the stated number of highest-ranking features from each feature selection method. In addition, the mean test errors using the highest-ranking features from aggregate votes are shown at the bottom (TOPN). (b) Lineplot showing the mean and dispersion of validation and test errors with the number of highest-ranking features from all feature selection methods. The faded areas show the 95% confidence intervals.

5.2 Patient skin doses

5.2.1 Measured skin doses and alert levels

In Publication III, alert levels for TAVI KAP and air kerma were proposed as 200 Gy·cm^2 and 2000 mGy, respectively. The highest measured MSD for TAVI was 2564 mGy. The second highest doses were measured for PCI, with the highest measured dose at 1507 mGy. TAVI and PCI MSD vs. KAP and air kerma are shown in Figure 17 and, as shown, PCI has a large KAP vs. MSD variation at high doses. In addition, Figure 17 hints at how TAVI doses are divided into two groups as the distance between the measurement points and the fitted line both above and below the line increases with KAP. Upon further analysis, two of the hospitals had much higher doses than the other three, as noted in Table 11, which shows the median and SD for MSD and the median for KAP values for the hospitals. Table 11 also shows the amount of collected Gafchromic film dosimetry data. Maximum MSD values were 377.27 mGy for CA, 941.68 mGy for PCI, 187.16 mGy for PI, 235.98 mGy for CRT, 415.35 mGy for AVNRT, 322.99 for AF and 4158 mGy for TAVI. Due to the interhospital variation for TAVI, hospital-specific alert levels were estimated at 160 Gy·cm^2 and 2000 mGy for KAP and air kerma, respectively, for both hospitals 1 and 2.

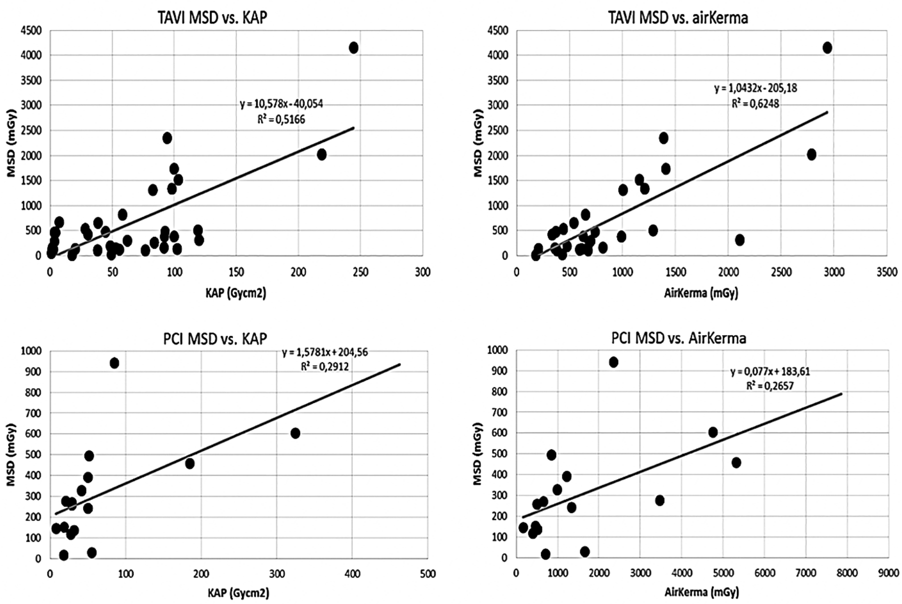

Figure 17. TAVI and PCI MSD vs. KAP and air kerma in Finland as published in Publication I.

Table 11. Median, amount of data (n) and SD for MSD (mSv) and median for KAP (Gy·cm^2) values for the hospitals in Publication III.

Hospital	Data	Median MSD (mGy)	Median KAP (Gy·cm^2)	MSD SD
Coronary procedures				
H1	12	114.1	55.4	15.5
H2	4	237.0	376.0	23.7
H3	19	284.2	272.4	34.3
H4	2	182.7	134.1	11.4
H5	4	131.9	102.6	24.4
H6	14	127.0	203.5	23.9
H7	8	97.2	48.8	21.7
Pacemaker implantations				
H1				
H2	1	62.8		
H3	10	119.8	48.2	1.3
H4	1	90.9		
H5	2	149.9	69.5	1.7
H6	2	140.2	97.2	14.5
Electrophysiological procedures				
H1				
H2	1	112.2		
H4	1	323.0		
H5	4	109.0	124.9	13.0
H6	4	142.4	156.0	23.3
TAVI procedures				
H1	10	1329.5	714.4	88.3
H2	6	1026.9	1519.0	80.0
H4[a]	4	289.7	127.0	92.1
H4[b]	9	164.0	211.8	24.4
H5	5	173.5	57.3	76.7
H6	4	126.2	131.9	29.0

[a] Siemens Axiom Artis dFA in 2016
[b] Siemens Artis Zeego Q in 2018

Table 12 compares measured skin doses to published values. As seen in the table, there is a large variation among studies but the results from this study are mostly very reasonable, with the exception of TAVI, which, as noted in Chapter 2, has very little published data.

5.2.2 Commercial skin dose mapping tools

GE DoseWatch and Siemens CareMonitor MSD estimates were compared to Gafchromic film dosimetry results in H1 and H4. These results are shown in Figure 18. For GE DoseWatch maximum local RPAK, a linear fitting of the data suggests the equation

$$MSD = 1.1092 \text{ x } RPAK + 7.4575, \tag{2}$$

and for Siemens CareMonitor, it suggests

$$MSD = 0.8582 \text{ x } RPAK + 49.811. \tag{3}$$

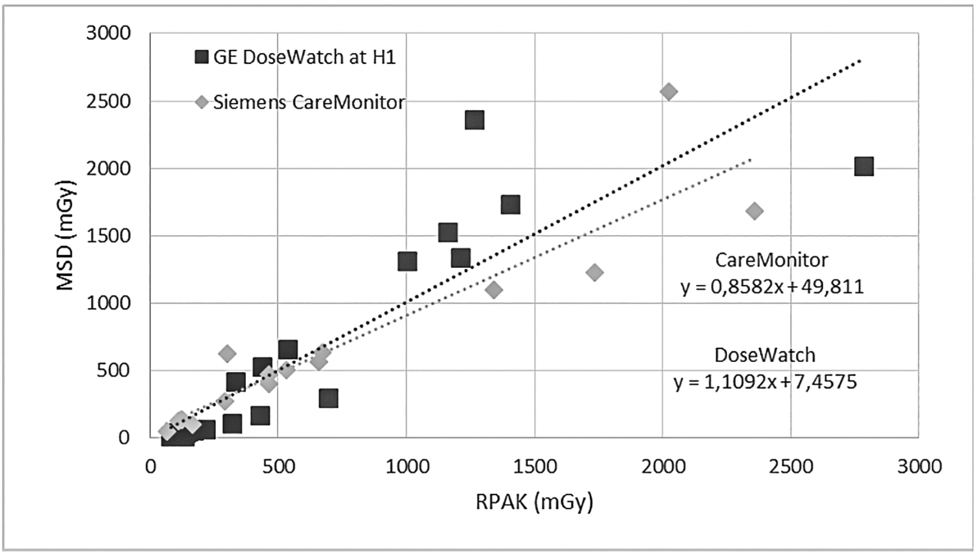

Figure 18. Measured MSD vs. maximum RPAK of GE DoseWatch (H1, n=20), Siemens CareMonitor at H1 (n=7) and Siemens CareMonitor at H4 (n=9) as published in Publication I.

Table 12. Comparison of mean MSD results (mGy) to various relevant publications as presented in Publication III. Amount of data in brackets.

	CA	PCI	PI	CRT	AVNRT	AF	TAVI
Publication III (mean)	116 (36)	405 (17)	96 (9)	122 (5)	159 (7)	210 (3)	624 (38)
a	159 (114)	505 (25)					
b	280 (44)	1030 (33)	30 (36)		170 (21)		
c	504 (2590)	976 (947)					
d	351 (9100)	1304 (5294)					
e		1482 (20)					
f	158 (90)						
g	103 (16)	526 (12)					
h	210 (39)	491 (25)					
i	264 (158)	596 (63)					
j							290 (15)

[a] (Quai et al., 2003)
[b] (Trianni et al., 2005)
[c] (Crowhurst et al., 2014), converted from RPAK to MSD using formula published by Teeuwisse et al. (Teeuwisse et al., 2001)
[d] (Pantos et al., 2009), total samples
[e] (Greffier et al., 2017)
f (Didier et al., 2019)
[g] (Pasquino et al., 2018)
[h] (Kulkarni et al., 2019)
[i] (Saeed, 2017)
[j] (Karambatsakidou et al., 2016)

5.2.3 Uncertainty analysis

Scanner long term repeatability uncertainty was estimated as 1.5% and 1.4% for Epson Expression 1600 Pro and Epson Expression 12000XL (Seiko Epson Corporation, Suwa, Japan), respectively. Scanner short-term repeatability uncertainty was 0.8% and 0.1% for the same scanners, respectively. The film dose rate response uncertainty was 0.6%, and film-to-film response uncertainty was 4.3%. Calibration fit uncertainty was 18.3% and 6.7% for the initial and newer calibrations, respectively. The differential analysis for the two calibrations showed that the slope of the newer calibration is 10.4% higher with the maximum difference at range 2.0 to 2.5 Gy. Reference air kerma uncertainty for the used calibration system was 1.0%.

Above uncertainty values were reasonably well in line with those reported by Farah et al. (Farah et al., 2015), with calibration fit uncertainty for the old calibration being the exception. Estimating the missing sources of uncertainty with literature values (Farah et al., 2015) (choice of fit for calibration 2%, amount and range of calibration data points 2% each, radiation quality dependence 2%, air kerma rate measurements 0.8% and beam uniformity 0.3%), total standard uncertainty was estimated as 19.3% for the initial calibration and 9.1% for the new calibration, within the 20% realistic estimate proposed by Farah et al. (Farah et al., 2015).

5.3 Heart organ doses related to TAVI

The mean heart dose from the CT scan was measured as 54.9 mGy and from the TAVI procedure as 25.5 mGy. The measurements' ranges and standard deviations are shown in Table 13. Table 14 shows relevant comparison values for a chest area CT angiography with a 64 slice scanner. However, none of the comparisons includes the body scan recommended by the Society of Cardiovascular Computed Tomography (Blanke et al., 2019). For a more accurate comparison, the heart organ dose can be estimated using literature values (Huda et al., 2010). Calculating the heart organ dose from a body CT scan with a dose level of Finnish DRL (STUK, 2013) results in 19.2 mGy, which explains much of the noted difference in Table 13. Calculating heart organ doses with the two CTDIvol values of the performed scans results in 59.6 mGy, which agrees well with the measurements (Huda et al., 2010).

Table 13. Measured heart organ doses related to a TAVI procedure in Turku university hospital.

Irradiation	Mean dose	Range	Standard deviation
CT scan	54.9 mGy	49.5 – 59.7 mGy	2.9 mGy
TAVI procedure	25.5 mGy	18.7 – 32.4 mGy	5.5 mGy

Heart organ doses for TAVI have not been previously published. For PCI, Brambilla et al. recently used the Monte Carlo program PCXMC 1.5 (STUK, Helsinki, Finland) (Servomaa and Tapiovaara, 1998) to calculate a median heart organ dose of 90.4 mGy based on data from 31 procedures with comparable KAP values (median 56.8 and 3rd quartile 76.5 Gy·cm^2) (Brambilla et al., 2017). Compagnone et al., on the other hand, reported median heart organ doses of 45.74 mGy (KAP 114.96 Gy·cm^2) for 75 PCI patients, similarly estimated with a Monte Carlo method (Compagnone et al., 2011). These differences in the obtained result of 25.5 mGy can likely be attributed to the observed variance in dose levels and used projections.

The background radiation dose in the annealed dosimeters was measured as 15.6 mGy. The dosimeter coefficient of variance was 19.9 %, which is in line with the low-dose (20 mGy) reproducibility value of 12.2% published by Manninen et al. (Manninen et al., 2012). Read-out uncertainty was measured as 0.2 %, which agrees with the literature values of 0.3% by Manninen et al. (Manninen et al., 2012) and 0.55% by Hsu et al. (Hsu et al., 2006).

Table 14. Comparison to relevant published organ doses (mGy) for CT angiography.

Study	Organ	Organ dose (mGy)	Type of scan	Area	kV	Slices	Gating
This study	Heart	54.9	Volume + helical	Heart + body	120	64	Diastolic
[a]	Heart	30.5	Helical	Heart	120	64	Diastolic
[a]	Heart	15.8	Volume	Heart	100	280	Diastolic
[b]	Heart	27.8	Helical	Heart	120	64	Retrospective
[b]	Lung	17.6	Helical	Heart	120	64	Retrospective
[c]	Lung	21.8	Volume	Heart	120	64	Prospective
[b]	Breast	25.5	Helical	Heart	120	64	Retrospective

[a] (Einstein et al., 2010)
[b] (Fink et al., 2011)
[c] (Khan et al., 2014)

6 Discussion

In cardiological procedures, the focus is always on patient survival and treatment of the possibly lethal disease. In all interventional use of radiation, decisions to utilize FL or cine are made instantaneously based on procedure status and learned best practices. In time, physicians' image quality preferences and personal priorities may change, e.g., with musculoskeletal pain due to ergonomic factors (Orme et al., 2015), expertise and stress level. As such, creating a safe and optimized culture of radiation hygiene is very important in interventional departments. In practice, this means continuous optimization, audits, and awareness of risks and good practices of all interventional staff. In this regard, guidelines prepared by the STUK (Järvinen et al., 2018a) are highly valuable to the contemporary Finnish IC scene.

In this thesis, the contemporary practice of radiation use in IC has been studied. This task is clearly visible in the KAP level variation between hospitals and countries, but it is intriguingly complex in its causes. Regardless of how this question might seem in some hospitals, it is important to approach it with a clear view of the whole situation.

The results presented in this thesis investigate the most relevant radiation risks to patients in contemporary cardiology and what issues affect it. As such, the results will help optimize clinical practice and support scientific work in the future.

6.1 Published diagnostic reference levels

In this thesis, the DRLs first published by the STUK (STUK, 2016) have been explored and compared to other published DRLs. With the data and methodology presented in both Publications I and II representing contemporary practice, the results provide a clear view into which procedures are the most important for radiation protection professionals and why. The results also emphasized the well-known need to regularly update DRLs because, by the time the new DRLs were published, the 2006 DRLs (STUK, 2005) were far higher than the dose levels of all participating hospitals.

In both Publications I and II, the DRLs were calculated as third-quartile values of the hospitals' medians for the quantity in question, in line with the ICRP recommendations (ICRP, 2017) and the STUK methodology for the new DRLs

(STUK, 2016). As mentioned in Chapter 2, traditionally, DRLs have been published as either the third-quartiles of the whole data or of the hospital medians, and this methodology is not always accurately reported (Georges et al., 2016). Compared to the dose levels calculated as the third-quartiles of the whole data, the new Finnish DRLs (medians of hospital third quartiles) were 30% lower on average. This difference, due to the methodology, was in line with the results published by Georges et al. (Georges et al., 2016).

DRLs are essential optimization tools, especially at the onset of the procedure, when extensive local dose data is not yet available. Of special interest before the study were the TAVI DRLs, which were among the first DRLs in the world. The resulting DRL for TAVI was the highest among the investigated procedures, and as such, the procedure was given further emphasis in the analysis. Similarly, the tentative KAP value for CRT procedures was among the first published in the world, and it was unfortunate that the amount of data did not allow for setting a DRL. However, even the tentative value proved interesting, as the value was so much higher than the DRL for PI. In the literature, CRT implantations are often treated as PI, but this is not advisable according to the published result. A similar effect was noticed in the electrophysiological procedures, which are also commonly grouped together in the literature (Simantirakis et al., 2013).

As explained in Chapter 2.2.1, estimating patient cancer risk requires significant estimations. Regardless, effective doses and absolute and relative cancer risks are a valuable tool in communicating radiation doses and their significance to the public. As shown in the results, radiation doses in cardiology vary between several and hundreds of $Gy \cdot cm^2$ for the various procedures considered in this study. Continuing with the example of cancer risk increase for PCI mentioned in the review of the literature, the absolute increase in cancer risk in Finland can be estimated to be between 0.002% and 0.2%. However, this estimation does not account for the significantly higher average age of IC patients compared to the populations used for effective dose calculations, and the actual increase might be even lower. Nonetheless, compared to the often-lifesaving benefits of the procedures, this increase from a single procedure can be considered small.

Comparing individual hospitals reveals the above-mentioned room for optimization also in Finland. Even as the national variation can be considered reasonable in Finland, TAVI and PCI procedures have an especially large interhospital dose variation, which likely reflects differences in practice. Whereas TAVI is a relatively new procedure in many hospitals, PCI is a traditional and well-known procedure, the variety of which supports the recommendation for the use of difficulty levels (ICRP, 2017).

In other procedures, compared to PCI and TAVI, the interhospital variation is reasonable with CA and CRT having the next-highest variations. However, compared to the non-interventional use of radiation in medicine with relatively well standardized studies, e.g., CT, the variation is relatively high. In Publication II, some electrophysiological procedures also had high variations between countries, which can likely be attributed to differences in procedure methodology.

Traditionally, differences in dose levels have also been largely attributed to angiosystem age (e.g. Gislason-Lee et al., 2016). However, as suggested by the results, this interpretation is insufficient. Even as new equipment potentially provides a significant boost in image quality and lower doses per pulse or frame, the magnitude of the boost varies and, sometimes, optimization work is carried out later, which disrupts the correlation. In addition, it is not always the case that these result in lower KAP, but rather in more demanding procedures instead. As such, even though angiosystem age had a statistically significant correlation to KAP in coronary and pacemaker procedures, the correlation was modest. In addition, TAVI procedures had a trend of slowly falling KAP, which might also disrupt the correlation for angiosystem age. The trend suggests a need for the re-evaluation of KAP levels in a few years and use of difficulty levels.

6.2 Predicting features and difficulty levels

IC patient KAP prediction and estimation of difficulty levels is a vast topic that is dependent on contemporary practice. The results obtained in this study can be an important part of a roadmap toward more accurate KAP comparison and personalized dosimetry. For coronary procedures, the division to CA and PCI and patient weight (ICRP, 2017) alone are not sufficient to predict IC KAP accurately. In addition, due to its subjectivity and inaccuracy of the scoring (Klein et al., 2008), using the AHA score to predict radiation use is relatively complex. Similarly, the use of patient weight or FT alone to describe procedure difficulty has been discouraged by the ICRP (ICRP, 2017) and the results presented in this thesis support this discouragement.

Besides CA/PCI and weight, multi-vessel disease, high pre-stenosis, gender, CTO or additional stenting can be seen relevant in predicting high radiation dose in coronary procedures. CTO in particular has a lower rank than expected based on studies such as (Pavlidis et al., 2016; Sakano et al., 2017; Tran et al., 2015) and Publication II. This may be due to the rarity of the CTO and whether all CTOs were noted correctly in the data. These results should be validated in a multi-center cohort study. In addition, the applied machine learning methodology can also be applied to other procedures, such as TAVIs, or optimization problems, such as which practices most affect KAP and what demographic or clinical factors affect these practices the most.

As for the obtained results on features predicting the use of radiation in TAVI procedures, it can be speculated that perhaps the main reason patient weight was the most descriptive factor (excluding fluoroscopy and cine KAP) was the low use of projections. With few options for better prosthesis visibility for bigger patients, better image quality templates are used. Unfortunately, if the protocols are not carefully optimized for different sizes of patients, this choice can significantly impact KAP.

In addition, as noted in the results for skin dosimetry, all collected TAVI doses, including KAP, were divided into two groups with two of the hospitals having higher doses than the other three. According to the performing cardiologists, this result was likely due to differences in methodology and access route. Likely, as suggested in Publication III, the result was partly because of the amount of data, but along with image quality and the level of protocol optimization, a number of other aspects also affect this variation, i.e., used techniques, distribution and optimized use of collimation, cine, zoom and 3D imaging also affect this variation. As such, TAVI procedures are a good subject for further studies on dose prediction.

6.3 Patient skin doses

In the results, Finnish IC skin doses and the available methods to monitor them have been presented. The highest skin doses were measured in TAVIs and alert levels of 200 $Gy \cdot cm^2$ for KAP and 2 Gy for air kerma were proposed for them. In the Finnish interventional use of radiation, a traditional alert level of 200 $Gy \cdot cm^2$ for early erythema has been used in many hospitals and departments in various diagnostic and therapeutic treatments. Based on the results presented in this thesis, this alert level is relatively accurate even today. Considering the KAP level and modest variation of projection, the resulting skin doses in TAVIs were not a surprise. With the exception of PCI, other procedures in IC are unlikely to exceed the 2 Gy level for early transient erythema.

Compared to other published results (noted in Chapter 2.2.4 as well as Publication III), the measured Gafchromic film dosimetry MSD values are reasonable. Although the measured mean doses are relatively low compared to the published limits for erythema (Balter et al., 2010), it should be recognized that it is entirely possible for individual cardiological procedures to have much higher doses, especially if the patient suffers from chronic total occlusion (Pavlidis et al., 2016; Tran et al., 2015). This was also the case in this study, as the noted maximum MSDs were much larger than the hospital medians.

The noted interhospital variation in TAVI procedures in Publication III was interpreted to suggest a need for hospital specific alert levels as earlier recommended by Järvinen et al. (Järvinen et al., 2018b). As such, indicative hospital specific alert levels were estimated for two of the participating hospitals with significantly lower KAP levels (160 Gy·cm^2 vs. 200 Gy·cm^2). Besides KAP level, the most significant factor in this result is the use of projections, which was modest in the two hospitals. Relevant personnel in both hospitals were noticed of the result.

In practice, the optimal use of skin dose estimates is the immediate oral and written relaying of information to patient and health records. Although the above alert level of 200 Gy·cm^2 is sufficiently accurate for general purposes, for individual patients and procedures, the variance in the MSD vs. KAP results is huge and is mainly attributable to changes in the use of projections. This and other relevant parameters are commonly considered by commercial skin dose mapping tools. As such, they can be seen to have great potential for personalized dosimetry. However, the tested mapping tools also have significant variations compared to the measured MSDs. As such, more information on vendor algorithms and estimations especially on patient geometry in various procedures should be publicly available and more independent studies on them should be carried out.

Total uncertainty of the measurements was estimated to be well within the proposed level of 20% by Farah et al. (Farah et al., 2015). The largest single uncertainty was estimated to result from calibration fit, which comprised of 95% of the total error for the initial calibration. For the newer calibration, this error was much more reasonable. The main reason for the big fit uncertainty for the initial calibration was that there are only five data points. An increasing number of data points and utilizing RQR7 instead of RQR5 would improve the calibration in the future.

6.4 Heart organ doses related to TAVI

Heart organ doses due to related CT scans and TAVI procedures were simulated and measured after the work on the publications was completed. Although unpublished, these measurements add to the comprehensive nature of the study and the breadth of utilized methodologies.

Even as CTA DLPs have been reported to have fallen internationally by 80% in the past decade (Stocker et al., 2018), the measured heart doses were quite surprisingly mainly comprised of dose from the CT scan (68% of the total dose). Compared to new guidelines from the Society of Cardiovascular Computed Tomography (Blanke et al., 2019), the protocol used by the Turku PET Centre deviated by performing the gated heart scan with a volume scan method and by its method of gating. With a 64-slice scanner, a helical acquisition with a retrospectively ECG-gated image reconstruction is recommended. With diastolic gating, aortic root dimensions are commonly smaller than in the systole, and systolic imaging is recommended (Blanke et al., 2019).

Besides these deviations from the recommendations, the results also suggest looking into the image quality of the scans, even after accounting for the body scan. Accordingly, the likely need for the optimization of the CT protocol has been raised with the medical physicists at the Turku PET Centre and the cardiologist responsible for them. However, it should be noted that the CT scan is a crucial part of the lifesaving procedure for relatively elderly patients, whose prognosis without a successful procedure is not very good. Thus, optimization that interferes with the procedures should be avoided.

Compared to the CT scan, the heart dose from the TAVI procedure itself had a larger standard deviation and range, which can be interpreted to result from the positioning of the dosimeters and from far less projections. In comparison to the PCI literature values, the measured TAVI procedure heart organ dose was small. However, due to only a few published results and differences in procedure and measurement methodologies, these comparisons are quite rough.

Compared to typical organ doses from diagnostic studies or angiographic procedures, the total heart organ dose of 80.4 mGy can be relatively high. However, due to TAVI's lifesaving nature, some perspective should perhaps be drawn from radiation therapy, in which heart organ doses below 40 Gy are often considered safe (Grimm et al., 2011).

6.5 Future prospects of radiation use in cardiology

In the future, personalized dosimetry is likely to develop and more and more sophisticated and accurate methods to evaluate and optimize radiation doses will emerge. This will apply to procedure KAP, skin doses, and procedure staff doses as well as to other medical uses of radiation.

Beyond dosimetric advances, the image quality of angiographic systems is likely to keep increasing with software and hardware innovations. Angiographic systems are bound by the temporal resolution desired by the doctors, and this has long set limits as to what kinds of image quality algorithms can be implemented. To circumvent them, various sophisticated techniques to optimize and speed up the calculations have been steadily introduced to the market and with the pace image quality algorithms have been developing, even algorithms utilizing some forms of iterative reconstruction or machine learning should not be considered as impossible to implement in the future, even in angiography. Likewise, technological advances regarding both X-ray detection and output will continue to play an important role in improving image quality and lowering the required radiation dose. Lastly, the use of shielding and its targeting will likely also improve resulting in both lower staff exposure and lower physical burden.

These changes will be the most pronounced in the most complex procedures, where most radiation is used. However, with the help of optimization tools and methodologies such as those presented in this thesis, it is quite possible that some of the effects will also affect how radiation is used in more common cardiological procedures today. As such, to keep up, monitoring and optimizing the use of radiation in this field is a task that will likely continue to evolve and accelerate for the foreseeable future.

Thanks to multinational groups and programs, such as the European radiation dosimetry group (EURADOS) and European Joint Programme for the Integration of Radiation Protection Research (CONCERT), scientific research in the field already has and will continue to improve. With well funded and organized scientific projects such as the ongoing Implications of Medical Low Dose Radiation Exposure (MEDIRAD) (Cardis et al., 2017) and Validation and Estimation of Radiation skin Dose in Interventional Cardiology (VERIDIC) (Malchair et al., 2018), knowledge on radiation protection and its optimal implementation will continue to increase. What we do with that knowledge largely defines us medical physicist working in the field.

7 Summary/Conclusions

In this study, patient exposure to radiation in IC has been studied in the Publications and the measurements of KAP, skin doses and TAVI heart organ doses. Radiation dose levels in contemporary practice in Finland have been shown to be relatively low compared to many European countries. In all participating countries, the dose variation was significant, especially in TAVI and PCI procedures. In this study, features explaining this variation in PCI procedures were explored, and patient weight, multi-vessel disease, high pre-stenosis, gender, CTO and additional stenting indicated a possible high radiation dose.

The highest doses in contemporary IC in Finland and Europe are in TAVIs and PCIs, and skin erythemas can also be concluded to be highly unlikely in any other IC procedures. Especially TAVI procedures contemporarily warrant alert levels, such as those recommended in this study. However, algorithms such as GE DoseWatch and Siemens CareMonitor appear highly promising in estimating patient skin dose and are likely to prove accurate and common enough to replace KAP or air kerma alert levels in the future.

Heart organ doses in TAVI appear to be significantly increased by the necessary CT scan before the procedure, and the need and ways of optimizing it have been discussed in this study. With careful optimization, this increase can be diminished.

Acknowledgements

There are many I wish to thank. For helping me grow. For helping me learn. For supporting me. Naturally, I wish to thank my principal supervisor, Joanna Sierpowska, who came up with the project and oversaw it from the beginning to the end. Mika Teräs, my local supervisor and boss, for understanding me, what I have been through and what this thesis has meant to me. And supporting me all the way. Teemu Siiskonen from the STUK, for teaching me so much, starting from more exact scientific thought in radiation dosimetry to remaining steadfast and calm. Visa Suomi for his professionalism, expertise on the difficult topics of machine learning and latex, and for his friendship.

This research would likely not have been possible without funding from Turku University Hospital's EVO grants and the Turku Heart Centre's crucial support in data, expertise, understanding and friendship. Without the support of practically all the people at the interventional cardiology department, this thesis would have been a much more difficult and gruesome task. Especially, I wish to thank Tuomas Kiviniemi, Mikko Pietilä, Antti Ylitalo, Juho Tammi, Sirpa Hirvisuo, Kristiina Wiberg, Suvi Koski, Juha Lund and Tiina Salo for teaching me so much about the use of radiation in cardiology and the relevant procedures.

Also crucial were all the people who supported me with data and expertise in the publications: Hanna Matikka, Eini Niskanen, Saija Hurme, Heli Larjava, Timo Mäkelä, Satu Strengell, Markku Eskola, Teuvo Parviainen, Elina Hallinen, Markku Pirinen and Antti Kivelä.

My colleagues, for their support in both fully and less professional matters. I hope we all find peace, inspiration and friendship, wherever we may be. Hannele, Lasse, Heli, Jani, Jalmari, Jarkko, and many others.

And last, but perhaps most importantly, I wish to express my sincere gratitude to the people I've been blessed to have close to me. Huỳnh. Family and friends. Without you, I wouldn't be here. Today and tomorrow. Thank you.

References

Airaksinen, J., Aalto-Setälä, K., Hartikainen, J., Huikuri, H., Laine, M., Lommi, J., Raatikainen, P., and Saraste, A. (2016). *Kardiologia*. Duodecim.

Alnawaf, H., Cheung, T., Butson, M. J., and Yu, P. K. N. (2010). Absorption spectra response of xrqa radiochromic film to x-ray radiation. *Radiation measurements*, 45(1):129-132.

Amano, M., Nishitani, H., Kohno, S., Yasutomo, M., Miyoshi, H., and Yagi, H. (2002). Measurement of patient skin dose in interventional radiology using radiochromic reflecting-type sheet films. *Nippon Hoshasen Gijutsu Gakkai Zasshi*, 58(3):420-423.

Amano, M., Nishitani, H., Kohno, S., Yasutomo, M., Miyoshi, H., and Yagi, H. (2003). Patient skin dose in interventional radiology using radiochromic dosimetry film. *Nippon Hoshasen Gijutsu Gakkai Zasshi*, 59(1):121-129.

Amano, M., Nishitani, H., Kohno, S., Yasutomo, M., Miyoshi, H., and Yagi, H. (2003). Patient skin dose in interventional radiology using radiochromic dosimetry film. *Nippon Hoshasen Gijutsu Gakkai Zasshi*, 59(1):121-129.

Amano, M., Nishitani, H., Kohno, S., Yasutomo, M., Miyoshi, H., and Yagi, H. (2003). Patient skin dose in interventional radiology using radiochromic dosimetry film. *Nippon Hoshasen Gijutsu Gakkai Zasshi*, 59(1):121-129.

Andreo, P. Monte Carlo techniques in medical radiation physics. *Physics in Medicine and Biology*, 36(7):861.

Ashley, E. A. and Niebauer, J. (2004). *Cardiology explained*. Remedica.

BAG (2018). Wegleitung r-06-05 diagnostische referenzwerte (drw) für interventionelle radiologische anwendungen.

Balter, S., Hopewell, J. W., Miller, D. L., Wagner, L. K., and Zelefsky, M. J. (2010). Fluoroscopically guided interventional procedures: a review of radiation effects on patients' skin and hair. *Radiology*, 254(2):326-341.

Bapat, V., Khawaja, M. Z., Attia, R., Narayana, A., Wilson, K., Macgillivray, K., Young, C., Hancock, J., Redwood, S., and Thomas, M. (2012). Transaortic transcatheter aortic valve implantation using edwards sapien valve. *Catheterization and Cardiovascular Interventions*, 79(5):733-740.

Beam, A. L. and Kohane, I. S. (2018). Big data and machine learning in health care. *Jama*, 319(13):1317-1318.

Blackledge, H. M. and Squire, I. B. (2009). Improving long-term outcomes following coronary artery bypass graft or percutaneous coronary revascularisation: results from a large, population-based cohort with first intervention 1995-2004. *Heart*, 95(4):304-311.

Blanke, P., Weir-McCall, J. R., Achenbach, S., Delgado, V., Hausleiter, J., Jilaihawi, H., Marwan, M., Norgaard, B. L., Piazza, N., Schoenhagen, P., and Leipsic, J. A. (2019). Computed tomography imaging in the context of transcatheter aortic valve implantation (tavi) / transcatheter aortic valve replacement (tavr): An expert consensus document of the society of cardiovascular computed tomography. *Journal of Cardiovascular Computed Tomography*, 13(1):1-20.

Brambilla, M., Cannillo, B., Matheoud, R., Compagnone, G., Rognoni, A., Bongo, A., and Carriero, A. (2017). Conversion factors of effective and equivalent organ doses with the air kerma area product in patients undergoing coronary angiography and percutaneous coronary interventions. *Physica Medica*, 42:189-196.

Brnic, Z., Krpan, T., Faj, D., Kubelka, D., Ramac, J. P., Posede, l. D., Steiner, R., Vidjak, V., Brni¢, V., Viskovi¢, K., and Baraban, V. (2009). Patient radiation doses in the most common interventional cardiology procedures in croatia: first results. *Radiation protection dosimetry*, 138(2):180-186.

Cadogan, M. (2014). AVNRT for two - available online https://lifeinthefastlane.com/avnrt-ecg/.

Camm, A. J., Lüscher, T. F., and Serruys, P. W. (2009). The ESC textbook of cardiovascular medicine. OXFORD university press

Cardis, E., Frija, G. (2017). Implications of medical low dose radiation exposure. Poster at ICRP, Paris.

Cheung, A. and Lichtenstein, K. M. (2012). Illustrated techniques for transapical aortic valve implantation. *Annals of cardiothoracic surgery*, 1(2):231-239.

Chida, K., Inaba, Y., Masuyama, H., Yanagawa, I., Mori, I., Saito, H., Maruoka, S., and Zuguchi, M. (2009). Evaluating the performance of a mosfet dosimeter at diagnostic x-ray energies for interventional radiology. *Radiological Physics and Technology*, 2(1):58-61.

Chmielak, Z., Demkow, M., Skowroński, J., Tyczyński, P., Zakrzewski, D., and Witkowski, A. (2017). Percutaneous mitral balloon valvuloplasty. Difficult mitral valve crossing. *Postepy kardiol interwencyjnej*, 13(4):347-348.

Clayton, B., Morgan-Hughes, G., and Roobottom, C. (2013). Transcatheter aortic valve insertion (tavi): a review. *British journal of radiology*, 87(1033):1-12.

Commission, I. E. et al. (1994). Medical diagnostic x-ray equipment-radiation conditions for use in the determination of characteristics. IEC 61267.

Compagnone, G., Ortolani, P., Domenichelli, S., Ovi, V., Califano, G., Dall'Ara, G., and Marzocchi, A. (2011). Effective and equivalent organ doses in patients undergoing coronary angiography and percutaneous coronary interventions. *Medical physics*, 38(4):2168-2175.

Cribier, A., Litzler, P. Y., Eltchaninoff, H., Godin, M., Tron, C., Bauer, F., and Bessou, J. P. (2009). Technique of transcatheter aortic valve implantation with the edwards-sapien heart valve using the transfemoral approach. *Herz Kardiovaskuläre Erkrankungen*, 34(5):347-356.

Crowhurst, J. A., Whitby, M., Thiele, D., Halligan, T., Westerink, A., Crown, S., and Milne, J. (2014). Radiation dose in coronary angiography and intervention: initial results from the establishment of a multi-centre diagnostic reference level in Queensland public hospitals. *Journal of medical radiation sciences*, 61(3):135-141.

Daoud, E. G. and Morady, F. (1998). Pathophysiology of atrial flutter. *Annual review of medicine*, 49(1):77-83.

D'Helft, C., McGee, A., Rainford, L., McFadden, S., Winder, J., Hughes, C., and Brennan, P. (2008). Proposed preliminary diagnostic reference levels for three common interventional cardiology procedures in ireland. *Radiation protection dosimetry*, 129(1-3):63-66.

Didier, R., Bourhis, D., Oueslati, C., Nasr, B., Le Ven, F., Noël, A., Jobic, Y., Damien, P., Pene-Baverez, D., Mansourati, J., et al. (2019). In vivo validation of dosemap software use in interventional cardiology with dosimetrics indicators and peak skin dose evaluation. *Catheterization and Cardiovascular Interventions*, 94(2):216-222.

Dietze, G., Harrison, J., and Menzel, H. (2009). Effective dose: a flawed concept that could and should be replaced. comments on a paper by dj brenner (br j radiol 2008; 81: 521-3). *The British journal of radiology*, 82(976):348-351.

Drummond, C. and Japkowicz, N. (2010). Warning: statistical benchmarking is addictive. kicking the habit in machine learning. Journal of Experimental & Theoretical Artificial Intelligence, 22(1):67-80.

DuBois, D. (1916). A formula to estimate the approximate surface area if height and body mass be known. *Arch Intern Med*, 17:863-871.

Einstein, A. J., Elliston, C. D., Arai, A. E., Chen, M. Y., Mather, R., Pearson, G. D. N., DeLaPaz, R. L., Nickoloff, E., Dutta, A., and Brenner, D. J. (2010). Radiation dose from single-heartbeat coronary ct angiography performed with a 320-detector row volume scanner. *Radiology*, 254(3):698-706.

Ellis, S. G., Roubin, G. S., King, S. B., Douglas, J. S., Weintraub, W. S., Thomas, R. G., and Cox, W. R. (1988). Angiographic and clinical predictors of acute closure after native vessel coronary angioplasty. *Circulation*, 88(2):372-379.

Ellis, S. G., Roubin, G. S., King, S. B., Douglas, J. S., Weintraub, W. S., Thomas, R. G., and Cox, W. R. (1990). Coronary morphologic and clinical determinants of procedural outcome with angioplasty for multivessel coronary disease. implications for patient selection. multivessel angioplasty prognosis study group. *Circulation*, 82(2):1193-1202.

Engström, G., Hedblad, B., Juul-Möller, S., Tydén, P., and Janzon, L. (2000). Cardiac arrhythmias and stroke: increased risk in men with high frequency of atrial ectopic beats. *Stroke*, 31(12):2925-2929.

ESC (2012). European guidelines on cardiovascular disease prevention in clinical practice (version 2012). *European journal of preventive cardiology*, 19(4):585-667.

ESC, Task Force Members, Montalescot, G., Sechtem, U., Achenbach, S., Andreotti, F., Arden, C., Budaj, A., Bugiardini, R., Crea, F., Cuisset, T., et al. (2013). 2013 ESC guidelines on the management of stable coronary artery disease: the task force on the management of stable coronary artery disease of the european society of cardiology. *European heart journal*, 34(38):2949-3003.

Farah, J., Trianni, A., Ciraj-Bjelac, O., Clairand, I., De Angelis, C., Delle Canne, S., Hadid, L., Huet, C., Jarvinen, H., Negri, A., et al. (2015). Characterization of xr-rv3 gafchromic® films in standard laboratory and in clinical conditions and means to evaluate uncertainties and reduce errors. *Medical physics*, 42(7):4211-4226.

Fink, C., Krissak, R., Henzler, T., Lechel, U., Brix, G., Takx, R. A. P., Nance, J. W., Abro, J. A., Schoenberg, S. O., and Schoepf, U. J. (2011). Radiation dose at coronary ct angiography: Second-generation dual-source ct versus single-source 64-mdct and first-generation dual-source ct. *American journal of radiology*, 196(5):550-557.

Fisher, D. R. and Fahey, F. H. (2017). Appropriate use of effective dose in radiation protection and risk assessment. *Health physics*, 113(2):102.

Foffa, I., Cresci, M., and Andreassi, M. G. (2009). Health risk and biological effects of cardiac ionising imaging: from epidemiology to genes. *International journal of environmental research and public health*, 6(6):1882-93.

Fokkema, M. L., James, S. K., Albertsson, P., Akerblom, A., Calais, F., Eriksson, P., Jensen, J., Nilsson, T., de Smet, B. J., Sjögren, I., et al. (2013). Population trends in percutaneous coronary intervention: 20-year results from the scaar (swedish coronary angiography and angioplasty registry). *Journal of the American College of Cardiology*, 61(12):1222-1230.

Furman, S., Hayes, D. L., and Holmes, D. R. (1989). *Clinical cardiac electrophysiology: techniques and interpretations*. Wiley-Blackwell.

Georges, J.-L., Belle, L., Etard, C., Azowa, J.-B., Albert, F., Pansieri, M., Monsegu, J., Barbou, F., Trouillet, C., Leddet, P., et al. (2016). Radiation doses to patients in interventional coronary procedures - estimation of updated national reference levels by dose audit. *Radiation protection dosimetry*, 175(1):17-25.

Gislason-Lee, A. J., Keeble, C., Malkin, C. J., Egleston, D., Bexon, J., Kengyelics, S. M., Blackman, D., and Davies, A. G. (2016). Impact of latest generation cardiac interventional x-ray equipment on patient image quality and radiation dose for trans-catheter aortic valve implantations. *The British journal of radiology*, 89(1067):20160269.

Gre-er, J., Ty, C. V. N., Bonniaud, G., Moliner, G., Ledermann, B., Schmutz, L., Cornillet, L., Cayla, G., Beregi, J., and Pereira, F. (2017). Assessment of peak skin dose in interventional cardiology: a comparison between gafchromic film and dosimetric software em. dose. *Physica Medica*, 38:16-22.

Grimm, J., LaCouture, T., Croce, R., Yeo, I., Zhu, Y., and Xue, J. (2011). Dose tolerance limits and dose volume histogram evaluation for stereotactic body radiotherapy. *Journal of applied clinical medical physics*, 12(2):267-292.

Guyon, I. and Elisseeff, A. (2003). An introduction to variable and feature selection. *Journal of machine learning research*, 3(Mar):1157-1182.

Haissaguerre, M., Warin, J. F., Lemetayer, P., Saoudi, N., Guillem, J. P., and Blanchot, P. (1989). Closed-chest ablation of retrograde conduction in patients with atrioventricular nodal reentrant tachycardia. *New England Journal of Medicine*, 320(7):426-433.

Hart, D., Hillier, M. C., and Wall, B. F. (2009). National reference doses for common radiographic, fluoroscopic and dental x-ray examinations in the UK. *British journal of radiology*, 82(973):1-12.

Hsu, S. M., Yang, H. W., Yeh, T. C., Hsu, W. L., Wu, C. H., Lu, C. C., Chen, W. L., and Huang, D. Y. C. (2007). Synthesis and physical characteristics of radiophotoluminescent glass dosimeters. *Radiation measurements*, 42(4-5):621-624.

Hsu, S. M., Yeh, S. H., Lin, M., and Chen, W. L. (2006). Comparison on characteristics of radiophotoluminescent glass dosemeters and thermoluminescent dosemeters. *Radiation protection dosimetry*, 119(1-4):327-331.

Huda, W., Rowlett, W. T., and Schoepf, U. J. (2010). Radiation dose at cardiac computed tomography facts and fiction. *Journal of thoracig imaging*, 25(3):204-212.

IAEA (2014). IAEA Basic Safety Standards.

ICRP (2007). The 2007 recommendations of the international commission on radiological protection. ICRP publication 103. *Annals of ICRP*, 37(2-4).

ICRP (2017). Diagnostic reference levels in medical imaging. ICRP publication 135. *Annals of ICRP*, 46(1).

Järvinen, H., Eskola, M., Hallinen, E., Järvinen, J., Kivelä, A., Mäkelä, T., Parviainen, T., Pirinen, M., Rissanen, T., Sierpowska, J., Siiskonen, T., and Vinni-Lappalainen, K. (2018a). *STUK Opastaa 2018: Säteilyn käytön turvallisuus kardiologiassa*. STUK.

Järvinen, H., Farah, J., Siiskonen, T., Ciraj-Bjelac, O., Dabin, J., Carinou, E., Domienik-Andrzejewska, J., Kluszczynski, D., Kneºevi¢, v., Kopec, R., Majer, M., Malchair, F., Negri, A., Pankowski, P., Sarmento, S., and Trianni, A. (2018b). Feasibility of setting up generic alert levels for maximum skin dose in fluoroscopically guided procedures. *Physics in Medicine*, 46:67-74.

Jin, H., Duftschmid, K. E., and Strachotinsky, C. (1992). *Investigation of a New LiF TLD Individual Dosimeter for Measuring Personal Dose Equivalent Hp(d) on Different Phantoms*. Austrian Research Centre Seibersdorf, Austria.

Josephson, M. E. (2008). *Clinical cardiac electrophysiology: techniques and interpretations*. Lippincott Williams & Wilkins.

Kaasalainen, T. (2015). *Optimizing computer tomography examinations by using anthropomorphic phantoms and MOSFET dosimeters*. University of Helsinki.

Kaier, K., Reinecke, H., Schmoor, C., Frankenstein, L., Vach, W., Hehn, P., Zirlik, A., Bode, C., Zehender, M., and Reinöhl, J. (2017). Learning curves among all patients undergoing transcatheter aortic valve implantation in germany: A retrospective observational study. *International journal of cardiology*, 235:17-21.

Karambatsakidou, A., Omar, A., Chehrazi, B., Rück, A., Scherp Nilsson, J., and Fransson, A. (2016). Skin dose, effective dose and related risk in transcatheter aortic valve implantation (tavi) procedures: is the cancer risk acceptable for younger patients? *Radiation protection dosimetry*, 169(1-4):225-231.

Khan, A. N., Shuaib, W., Nikolic, B., Khan, M. K., Kang, J., and Khosa, F. (2014). Absorbed radiation dose in radiosensitive organs using 64- and 320-row multidetector computed tomography: A comparative study. *Scientifica (Cairo)*, 2014.

Kiviniemi, T. O., Pietilä, A., Gunn, J. M., Aittokallio, J. M., Mähönen, M., Salomaa, V. V., and Niiranen, T. J. (2016). Trends in rates, patient selection and prognosis of coronary revascularisations in Finland between 1994 and 2013: the CVDR. *EuroIntervention*, 12(9):1117-1125.

Klein, L. W., Miller, D. L., Balter, S., Laskey, W., Naito, N., Haines, D., Ross, A., Mauro, M. A., and Goldstein, J. A. (2009). Occupational health hazards in the interventional laboratory: Time for a safer environment. *Catherization and cardiovascular interventions*, 250(2):538-544.

Knuuti, J. and Järvinen, J. (2014). Radiation exposure and the risk of cancer for interventional cardiologists and electrophysiologists. *European heart journal*, 35(10):599-604.

Kuck, K.-H., Brugada, J., Fürnkranz, A., Metzner, A., Ouyang, F., Chun, K. J., Elvan, A., Arentz, T., Bestehorn, K., Pocock, S. J., et al. (2016). Cryoballoon or radiofrequency ablation for paroxysmal atrial fibrillation. *New England Journal of Medicine*, 374(23):2235-2245.

Kulkarni, A. R., Akhilesh, P., Sharma, S. D., et al. (2019). Measurement of patient skin dose and establishment of local diagnostic reference levels for interventional cardiology procedures. *Radiation Protection and Environment*, 42(1):28.

Lee, J. H., Lin, M. S., Hsu, S. M., Chen, I. J., Chen, W. L., and Wang, C. F. (2009). Dosimertry characteristics and performance comparisons: environmental radiophotoluminescent glass dosemeters versus thermoluminescent dosemeters. *Radiation measurements*, 44(1):86-91.

Lee, K. W., Yang, Y., and Scheinman, M. M. (2005). Atrial flutter: a review of its history, mechanisms, clinical features, and current therapy. *Current problems in cardiology*, 30(3):121-167.

Lin, E. C. (2010). Radiation risk from medical imaging. *Mayo clinic proceedings*, 85(12):1142-1146.

Klein, L.W. and Krone, R.J. (2008). Angiographic characterization of lesion morphology are the aha / acc and scai lesion classifications still useful? *Cardiac Interventions Today*, July/August:44-49.

Lund, J., Saraste, A., and Airaksinen, J. (2012). Percutaneous left atrial appendage closure with minimal antithrombotic treatment in patients at very high risk of bleeding events. *Thrombosis research*, 30(3):194-195.

Malchair, F., Dabin, J., Deleu, M., Maccia, C., and Sans Merce, M. (2018). *D 9.141 - Standards for digital dose reporting*. WP9. The Concert EJP.

Manninen, A.-L. (2014). *Clinical applications of radiophotoluminescence (RPL) dosimetry in evaluation of patient radiation exposure in radiology: Determination of absorbed and effective dose*. University of Oulu.

Manninen, A.-L., Koivula, A., and Nieminen, M. T. (2012). The applicability of radiophotoluminescence dosemeter (rpld) for measuring medical radiation (mr) doses. *Radiation protection dosimetry*, 151(1):1-9.

Mantziari, A., Ziakas, A., Stavropoulos, G., and Styliadis, I. H. (2011). Clinical applications of intravascular ultrasound (ivus): experience from an academic high volume centre of northern greece. *Hippokratia*, 15(1):60-63.

McKeever, S. W. S., Moscovitch, M., and Townsend, P. D. (1995). *Thermoluminescence dosimetry materials: properties and uses*. United Kingdom: Nuclear Technology Publishing.

Mehra, A. and Mohan, B. (2015). Value of FFR in clinical practice. *Indian heart journal*, 67(1):77-80.

Miller, D. L., Balter, S., Cole, P. E., Lu, H. T., Berenstein, A., Albert, R., Schueler, B. A., Georgia, J. D., Noonan, P. T., Russell, E. J., et al. (2003a). Radiation doses in interventional radiology procedures: The RAD-IR study part II: skin dose. *Journal of vascular and interventional radiology*, 14(8):977-990.

Miller, D. L., Balter, S., Cole, P. E., Lu, H. T., Schueler, B. A., Geisinger, M., Berenstein, A., Albert, R., Georgia, J. D., Noonan, P. T., et al. (2003b). Radiation doses in interventional radiology procedures: the RAD-IR study part I: overall measures of dose. *Journal of vascular and interventional radiology*, 14(6):711-727.

Miller, D. L., Hilohi, C. M., and Spelic, D. C. (2012). Patient radiation doses in interventional cardiology in the us: advisory data sets and possible initial values for us reference levels. *Medical physics*, 39(10):6276-6286.

Niiniviita, H. (2017). *Estimation of radiation dose and image quality in pediatric and young adult computed tomography studies*. University of Turku.

Oberhauser, J. P., Hossainy, S., and Rapoza, R. J. (2009). Design principles and performance of bioresorbable polymeric vascular scaffolds. *EuroIntervention: journal of EuroPCR in* *collaboration with the Working Group on Interventional Cardiology of the European Society of Cardiology*, 5:F15-22.

Orme, N. M., Rihal, C. S., Gulati, R., Holmes, D. R., Lennon, R. J., Lewis, B. R., McPhail, I. R., Thielen, K. R., Pislaru, S. V., Sandhu, G. S., et al. (2015). Occupational health hazards of working in the interventional laboratory: a multisite case control study of physicians and allied staff. *Journal of the American College of Cardiology*, 65(8):820-826.

Padovani, R., Vano, E., Trianni, A., Bokou, C., Bosmans, H., Bor, D., Jankowski, J., Torbica, P., Kepler, K., Dowling, A., et al. (2008). Reference levels at european level for cardiac interventional procedures. *Radiation protection dosimetry*, 129(1-3):104-107.

Paile, W. (2002). Säteilyn terveysvaikutukset. STUK.

Pantos, I., Pataloukas, G., Katritsis, D. G., and Efstathopoulos, E. (2009). Patient radiation doses in interventional cardiology procedures. *Current cardiology review*, 5(1):1-11.

Pasquino, M., Cutaia, C., Poli, M., Valero, C., Peroni, G., De Benedictis, M., Petrucci, E., and Stasi, M. (2018). Patient's peak skin dose evaluation using gafchromic films in interventional cardiology procedures and its correlation with other dose indicators. *Physica Medica*, 53:103-107.

Pavlidis, A. N., Jones, D. A., Sirker, A., Mathur, A., and Smith, E. J. (2016). Reducing radiation in chronic total occlusion percutaneous coronary interventions. *Current cardiology reviews*, 12(1):12-17.

Pedregosa, F., Varoquaux, G., Gramfort, A., Michel, V., Thirion, B., Grisel, O., Blondel, M., Prettenhofer, P., Weiss, R., Dubourg, V., et al. (2011). Scikit-learn: Machine learning in python. *Journal of machine learning research*, 12(Oct):2825-2830.

Picano, E. and Vano, E. (2011). The radiation issue in cardiology. *Cardiovascular Ultrasound*, 9.

Quai, E., Padovani, R., Peterzol, A., Vano, E., Guibelalde, E., and Toivonen, M. (2003). *Maximum skin dose assessment in interventional cardiology: results in three different european hospitals*. European Congress of Radiology 2003.

Rah, J. E., Hong, J. Y., Kim, G. Y., Kim, Y. L., Shin, D. O., and Suh, T. (2009). A comparison of the dosimetric characteristics of a glass rod dosimeter and a thermoluminescent dosimeter for mailed dosimeter. *Radiation measurements*, 44(1):18-22.

Rasband, W. S. (2016). Imagej - available online https://imagej.nih.gov/ij/.

Rehani, M. M. (2007). Training of interventional cardiologists in radiation protection-the IAEA's initiatives. *International journal of cardiology*, 114(2):256-260.

Riesen, H. and Liu, Z. (2012). *Optical Storage Phosphors and Materials for Ionizing Radiation, Current Topics in Ionizing Radiation Research*. InTech.

Ryan, T. J., Faxon, D. P., Gunnar, R. M., Kennedy, J. W., King3rd, S. B., Loop, F. D., Peterson, K. L., Reeves, T. J., Williams, D. O., and WintersJr, W. L. (1988). Guidelines for percutaneous transluminal coronary angioplasty. *Circulation*, 78(2):486-502.

Sackett, D. L., Rosenberg, W. M. C., Gray, J. A. M., Haynes, R. B., and Richardson, W. S. (1996). Evidence based medicine: what it is and what it isn't. *BMJ*, 312(7023):71-2.

Saeed, M. (2017). Dose measurement using gafchromic film for patients undergoing interventional cardiology procedures. *Radiation protection dosimetry*, 174(1):109-112.

Sakano, T., Iwamoto, T., Kuribara, T., Sakamoto, H., Tajima, O., Hamano, Y., Maruyama, M., Kikuchi, T., Tsukamoto, A., and Kato, K. (2017). Survey of exposure dose during percutaneous coronary intervention for chronic total occlusion. *Nihon Hoshasen Gijutsu Gakkai zasshi*, 73(1):51-56.

Saukko, E., Henner, A., Nieminen, M. T., and Ahonen, S.-M. (2017). The establishment of local diagnostic reference levels in endoscopic retrograde cholangiopancreatography: a practical tool for the optimisation and for quality assurance management. *Radiation protection dosimetry*, 173(4):338-344.

Servomaa, A. and Tapiovaara, M. (1998). Organ dose calculation in medical x ray examinations by the program pcxmc. *Radiation Protection Dosimetry*, 80(1-3):213-219.

Sherif, M. A., Paranskaya, L., Yuecel, S., Kische, S., D'Ancona, G., Neuhausen-Abramkina, A., Ortak, J., Ince, H., and Öner, A. (2016). Mitraclip step by step; how to simplify the procedure. *Netherlands heart journal*, 25(2):125-130.

Simantirakis, G., Koukorava, C., Kalathaki, M., Pafilis, C., Kaisas, I., Economides, S., Hourdakis, C. J., Kamenopoulou, V., and Georgiou, E. (2013). Reference levels and patient doses in interventional cardiology procedures in greece. *European radiology*, 23(8):2324-2332.

Sipahi, I., Akay, M. H., Dagdelen, S., Blitz, A., and Alhan, C. (2014). Coronary artery bypass grafting vs percutaneous coronary intervention and long-term mortality and morbidity in multivessel disease: meta-analysis of randomized clinical trials of the arterial grafting and stenting era. *JAMA internal medicine*, 174(2):223-230.

Sosiaali- ja terveysministeriö (2018). Säteilylaki 859/2018 - available online https://www.finlex.fi/fi/laki/alkup/2018/20180859.

Statens strålevern (2010). Reviderte og nye nasjonale referanseverdier for røntgendiagnostiske undersøkelser per 2010.

Steinberg, D. H., Staubach, S., Franke, J., and Sievert, H. (2010). Defining structural heart disease in the adult patient: current scope, inherent challenges and future directions. *European Heart Journal Supplements*, 12:E2-E9.

Stocker, T. J., Heckner, M., Deseive, S., Leipsic, J., Chen, M., Rubinshtein, R., Hadamitzky, M., Bax, J. J., Grove, E., Lesser, E., Fang, X. M., P, M., Otton, J., Shin, S., and Hausleiter, J. (2018). Radiation dose reduction in cardiac ct: results from the prospective multicenter registry on radiation dose estimates of cardiac ct angiography in daily practice in 2017. *European heart journal*, 39(Supplement 1):2484.

STUK (2005). Päätös 27/310/05: Potilaan säteilyaltistuksen vertailutasot kardiologisessa radiologiassa.

STUK (2013). Päätös 2/3020/2013: Potilaan säteilyaltistuksen vertailutasot aikuisten tietokonetomografiatutkimuksissa.

STUK (2015). Päätös 9/3020/2015: Potilaan säteilyaltistuksen vertailutasot lasten tietokonetomografiatutkimuksissa.

STUK (2016). Päätös 15/3020/2016: Potilaan säteilyaltistuksen vertailutasot kardiologisessa radiologiassa.

STUK (2019). Use of radiation in health care - available online http://www.stuk.fi/web/en/topics/use-of-radiation-in-health-care.

Sun, X., Abaziz, A., and Yusof, A. (2013). Radiation-induced noncancer risks in interventional cardiology: Optimisation of procedures and staff and patient dose reduction. *BioMed research international*.

Teeuwisse, W., Geleijns, J., Broerse, J., Obermann, W., and Van Persijn Van Meerten, E. (2001). Patient and staff dose during ct guided biopsy, drainage and coagulation. *The British journal of radiology*, 74(884):720-726.

Terashima, M., Kaneda, H., and Suzuki, T. (2012). The role of optical coherence tomography in coronary intervention. *Korean journal of interventional medicine*, 27(1):1-12.

Tran, P., Phan, H., Shah, S. R., Latif, F., and Nguyen, T. (2015). Radiation safety during interventions of coronary chronic total occlusion. *Current Cardiology Reviews*, 11(4):314-316.

Trianni, A., Chizzola, G., Toh, H., Quai, E., Cragnolini, E., Bernardi, G., Proclemer, A., and Padovani, R. (2005). Patient skin dosimetry in haemodynamic and electrophysiology interventional cardiology. *Radiation protection dosimetry*, 117(1-3):241-246.

Vano, E., Kleiman, N. J., Duran, A., Rehani, M. M., Echeverri, D., and Cabrera, M. (2010). Radiation cataract risk in interventional cardiology personnel. *Radiation research*, 174(4):490-495.

Vijayalakshmi, Kand Kelly, D., Chapple, C.-L., Williams, D., Wright, R., Stewart, M. J., Hall, J. A., Sutton, A., Davies, A., Haywood, J., and de Belder, M. A. (2007). Cardiac catheterisation: radiation doses and lifetime risk of malignancy. *Heart*, 93(3):370-371.

Wall, B. F. and Hart, D. (1997). Revised radiation doses for typical x-ray examinations. report on a recent review of doses to patients from medical xray examinations in the UK by NRPB national radiological protection board. *The British journal of radiology*, 70(833):437-439.

Wall, B. F. and Shrimpton, P. C. (1998). The historical development of reference doses in diagnostic radiology. *Radiation protection dosimetry*, 80(1-3):15-20.

Zotova, R., Vassileva, J., Hristova, J., Pirinen, M., and Järvinen, H. (2012). A national patient dose survey and setting reference levels for interventional radiology in Bulgaria. *European Radiology*, 22(6):1240-1249.

UNIVERSITY
OF TURKU

Painosalama Oy, Turku, Finland 2020

ISBN 978-951-29-8068-0 (PRINT)
ISBN 978-951-29-8069-7 (PDF)
ISSN 0355-9483 (Print)
ISSN 2343-3213 (Online)